Plant Stress 14 (2024) 100603

Contents lists available at ScienceDirect

Plant Stress

journal homepage: www.sciencedirect.com/journal/plant-stress

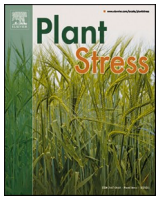

Early and late responses to Fusarium Head blight in durum wheat: Focus on phenylpropanoid biosynthetic pathway

Linda Felici [a,*], Federica Castellani [b], Sara Francesconi [a], Matteo Vitali [b], Francesco Sestili [a], Giorgio Mariano Balestra [a,*]

[a] University of Tuscia, Department of Agriculture and Forest Sciences (DAFNE), Via San Camillo de Lellis SNC, Viterbo, Italy
[b] Department of Public Health and Infectious Diseases, University of Rome La Sapienza, Rome, Italy

ARTICLE INFO

Keywords:
Triticum turgidum L. subsp. *Durum*
Anthocyanins
Flavonoids
Phenolic acids
Fusarium graminearum
Pigmented grains

ABSTRACT

Durum wheat is among the cereal crops most susceptible to Fusarium Head Blight (FHB), a fungal disease that can lead to significant yield losses. Despite this, only limited research efforts have been directed towards understanding FHB resistance in durum wheat. Wheat grains naturally contain phenolic compounds, and anthocyanins are particularly present in the so-called pigmented wheat genotypes, such as purple pericarp ones. In this study the effects of the biotic stress caused by *Fusarium graminearum* infection on phenylpropanoid biosynthetic pathway in durum wheat spikes were explored, considering three genotypes with different susceptibility (including a purple pericarp genotype), and two time points (an early stage time point: 2 days post infection, and a late stage time point: 21 days post infection). At early infection stage, the *F. graminearum* infection triggered upregulation of all the considered genes involved in the phenylpropanoid pathway in the resistant genotype, while, in the purple pericarp genotype, the infection caused an increase in quercetin accumulation in the soluble fraction of spike extract. At late infection stage, the infection caused (in all the genotypes) a degradation of secondary cell wall and the release of the hydroxycinnamic acids esterified with arabinoxylans (ferulic acid and *p*-coumaric acid) and lignin-derived monomers (vanillic acid). Furthermore, chalcone synthase gene (*CHS*) and the transcription factor *Ppm1* (Purple pericarp MYB 1) were boosted in the pigmented genotype due to infection at late infection stage. These findings contribute to the understanding of host-pathogen interactions for future breeding programs focused on improving FHB resistance in durum wheat varieties, with a particular focus on pigmented genotypes.

1. Introduction

Phenylpropanoids (or phenolic compounds) are natural products abundantly produced by plants (Durazzo et al., 2019), which possess several biochemical properties, such as reducing capacity, binding properties (Belščak-Cvitanović et al. 2018), anti-inflammatory, antibacterial, antifungal, antigenotoxic (Daglia 2012) and antioxidant activity (Oufensou et al. 2020; Gautier et al. 2020; Brainina et al. 2019). Phenylpropanoid biosynthesis in plants has been studied in-depth. It begins with the deamination of l-phenylalanine by l-phenylalanine ammonia-lyase (PAL), followed by reactions catalyzed by 4CL (4-coumarate-coenzyme A ligase, which catalyzes the formation of CoA thioesters of hydroxycinnamic acids) and C4H (cinnamate 4-hydroxylase, which leads to the hydroxylation at the C4 position of the aromatic ring). The pathway then branches out into several routes. The 3′-hydroxylation of coumaroyl quinate/shikimate, followed by the reactions catalyzed by ferulate 5-hydroxylase (F5H) and caffeic acid O-methyltransferase (COMT), lead to the production of lignin monomers and then lignin (Goujon et al. 2003). The production of naringenin chalcone from *p*-coumaroyl-CoA and malonyl-CoA molecules by CHS (chalcone synthase) starts the flavonoid branch of the pathway. This branch continues through reactions catalyzed by chalcone isomerase (CHI) to form trihydroxyflavanones, further hydroxylated by flavanone-3-hydroxylase (F3H) to form dihydroflavanols. Dihydroflavanols are then reduced by dihydroflavonol 4-reductase (DFR) to produce colorless anthocyanin glycosides, which are subsequently catalyzed by anthocyanidin synthase (ANS) to produce colored anthocyanins (Sunil and Shetty 2022). Dihydroflavanols can be the substrate of other enzymes, such as the FLS (flavonol synthase) producing flavones like kaempferol or quercetin (Gebhardt et al. 2007). The genes involved in phenylpropanoid

* Corresponding authors.
E-mail addresses: felici@unitus.it (L. Felici), balestra@unitus.it (G.M. Balestra).

https://doi.org/10.1016/j.stress.2024.100603
Received 21 March 2024; Received in revised form 22 August 2024; Accepted 13 September 2024
Available online 18 September 2024

biosynthesis can be divided into structural genes (functional genes, which encode for the above-mentioned enzymes) and regulatory genes. The expression of structural genes during anthocyanin biosynthesis is directly regulated by the MYB-bHLH-WDR complex (Liu et al. 2021), which varies in the different plant species.

Wheat grains are surely an important source of carbohydrates, but they also naturally contain several antioxidant bioactive compounds, such as carotenoids, tocopherols and phenolic compounds (Abdel-Aal and Rabalski 2008). Anthocyanins are particularly accumulated in the so-called pigmented wheat genotypes. These cultivars have blue to blue-black, and red to purple grains which could be distinguished in purple pericarp (expressing purple color in pericarp layer), blue aleurone (rich in anthocyanins in the aleurone layer), and black (having both pigmented pericarp and aleurone layers) genotypes (Böhmdorfer et al. 2018). Although their distribution is currently limited, interest in these genotypes is increasing due to their nutritional value (Hu et al. 2007; Cory et al. 2018; Singh et al. 2020) and for the function of polyphenols in plant life. Indeed, pigments, anthocyanins and phenolic compounds are essential for plants, where they play a role in senescence regulation, internal and external signaling, reproduction and reaction to several abiotic and biotic stresses (Wagay et al. 2020; Li and Ahammed 2023).

More in detail, several studies highlighted as phenylpropanoids and flavonoids are involved in abiotic stress tolerance. Drought tolerance could be influenced by both phenylpropanoids structural genes (such as *TaCHS, TaCHI, TaF3H, TaFNS, TaFLS,TaDFR*, and *TaANS*) (Ma et al., 2014; Niu et al., 2023) and regulatory genes (Wei et al., 2017). Su et al. (2019) found that transcriptional regulation of zeatin, brassinosteroid and flavonoid biosynthesis pathways may play an important role in wheat's heat tolerance. Furthermore, flavonoids are UV-B absorbing compounds (Feng et al., 2007) and may be impacted by intense radiation (Gondor et al., 2014). Moreover, different studies highlighted as bread wheat genotypes having colored grains show enhanced stress tolerance. For instance, the deep purple inbred line K4191 showed salinity stress tolerance (Hong et al., 2024), and the dark seed coat Recombinant Inbred Lines (RILs) investigated by Calderon Flores et al. (2021) were highly responsive to cold acclimation.

Regarding biotic stress, different studies showed that an increase in anthocyanin content or an alteration in plants phenylpropanoids biosynthetic pathway affects resistance response to bacterial (Wegener and Jansen 2007; Lei et al. 2018) and fungal pathogens (Zhang et al. 2013; Sivankalyani et al. 2016; Flachowsky et al. 2010). Among the main biotic stresses of cereals, Fusarium Head Blight (FHB) stands out (McMullen et al. 2012). This disease is caused by several hemibiotrophic fungal pathogens belonging to *Fusarium* spp. genera, causing bleaching and necrosis on the spikes. Infection occurs during flowering through stomata or other openings and then the mycelium spreads along the rachis, leading to kernel disruption and mycotoxins contamination (Mielniczuk and Skwaryło-Bednarz 2020).

Flavonoids and phenylpropanoids may play different roles in wheat-*Fusarium* interaction, including direct effect against the pathogen. Numerous studies have shown that phenolic acids and phenolic acid-rich plant extracts can reduce *Fusarium* spp. fungal growth and trichothecene production in vitro (Aristimuño Ficoseco et al., 2014; A.-L. Boutigny et al., 2009; A. Boutigny et al., 2010; Gauthier et al., 2016; Lalak-Kańczugowska et al., 2023; Martínez-Fraca et al., 2022; Shirai and Tanaka, 2024). The mode of action of these compounds usually involves regulation of fungal gene expression (A. Boutigny et al., 2010; Gautier et al., 2020) and alteration of oxidative balance (Savignac et al., 2023). The most studied secondary plant metabolites for direct antifungal and anti-mycotoxins action are phenolic acids (mainly caffeic acid, p-coumaric acid, ferulic acid, sinapic acid, vanillic acids, syringic acid), carotenoids (zeaxanthin) and some flavonoids (rutin, quercetin, naringenin, chlorogenic acid).

All of these compounds exist in cereals in both soluble (free) and insoluble (cell wall-bound) forms (Paznocht et al., 2020). Many of the cell wall-bound compounds are constitutively present (Saulnier et al., 2012), contributing to the preformed resistance mechanisms of wheat against fungal infections. Other authors showed as cell wall composition contribute to FHB resistance (Picot et al., 2013). However, biosynthesis of phenylpropanoids and flavonoids could be also actively stimulated by the infection, enhancing the inducible resistance mechanisms (Gunnaiah and Kushalappa, 2014). Recognition of the intruder leads to signaling cascades stimulating an increase of cell wall thickness, cell wall cross-linking, lignification, and enrichment with phenolics (e.g. ferulic acid, p-coumaric acid) (Walter et al., 2010). Additionally, phenylpropanoids and flavonoids are known for their notable antioxidant activity, which means their ability to inhibit (reduce) all molecules having high Ox/Red potential (Brainina et al., 2019). Because infection of plants by various pathogens is accompanied by oxidative stress, the presence of phenolic acids, flavonoids and anthocyanins in a plant may have a positive effect on the resistance to biotic stress (Shoeva et al., 2017).

Furthermore, phenylpropanoid and flavonoid pathways are interconnected with the synthesis of salicylic acid, the plant hormone responsible for activating systemic acquired resistance (SAR) (Hao et al. 2019). Salicylic acid (SA) is a small phenolic compound that regulates plant growth and development (Rivas-San Vicente and Plasencia, 2011); it also serves as a critical signal to activate the expression of disease resistance genes (An and Mou, 2011). The salicylic acid (SA) signal pathway is associated with FHB resistance at the early infection stage (Makandar et al., 2011). Conversely, jasmonic acid (JA) promotes the infection by constraining the SA signaling pathway during the early stage of infection and promotes resistance during the later stages of infection (Whitney et al., 2022).

Among the cereal crops, durum wheat (*Triticum turgidum* L. subsp. *durum* (Desf.) Husn.), used to produce semolina and several traditional food products in the Mediterranean basin (Conte et al. 2021; Boukid 2021), is particularly susceptible to FHB (Gaikpa et al. 2020). Resistance to FHB is a complex trait, regulated by several Quantitative Trait Loci (QTLs). Different resistance type have been described, such as type I resistance (resistance to first fungal penetration) or type II resistance (resistance to fungal spread into the rachis) (Mesterhazy, 2020). There are currently no fully FHB-resistant durum wheat cultivars available. However, FHB-resistant durum wheat experimental lines have been developed, such as DBC-480 (Prat et al., 2017), harboring the introgression of the resistant quantitative trait locus *Fhb1* from Sumai-3. Function of *Fhb1* locus remain controversial (Hao et al., 2020) and specific studies about DBC-480 resistance mechanism are lacking. Even though, different authors proposed that phenylpropanoids may play a role in Sumai-3 resistance. Zhao et al. (2022) suggested that flavonoids and its derivatives might contribute significantly to black necrotic lesion formation in FHB-resistant plants. Gunnaiah and Kushalappa (2014) founds several phenylpropanoids such as kaempferol, naringenin, catechin, cyanidin, and other flavonoids being resistance related induced or resistance related constitutive compounds in Sumai-3. However, other studies hypothesized that phenylpropanoids may be the basis resistance, but other metabolites promoting resistance are needed in resistant genotypes in addition to phenylpropanoid compounds (Dong et al., 2023).

To date, only a limited number of studies have addressed the determination of FHB resistance level in pigmented wheat genotypes. Gozzi et al. (2023) correlated anthocyanins content and a reduced mycotoxins accumulation in twelve varieties of pigmented common wheat (*T. aestivum* L. spp. *aestivum* L.), while Trávníčková et al. (2024) investigated 25 colored-grain wheat cultivars, highlighting an association between Fusarium head blight resistance and grain color, but with a high degree of instability of the traits studied in each cultivation year. Currently, there are no data on resistance or susceptibility to FHB in pigmented durum wheat genotypes. Our previous study (Felici et al., 2024) investigated some physiological and morphological traits associated with Fusarium head blight response in Purple durum, a purple pericarp durum wheat genotype, which resulted FHB-susceptible, but

able to maintain a stable grain number regardless the infection.

Different biochemical studies have been attempted to decipher the biochemical defenses that contribute to FHB, through comparative metabolites composition of resistant and susceptible varieties (Atanasova-Penichon et al., 2016). At the same time, different gene expression analysis were applied to study wheat lines with contrasting levels of head blight resistance after *Fusarium graminearum* inoculation (Steiner et al., 2009) and with particular phenylpropanoid pathway for investigating phenylpropanoid-based resistance to FHB (Funnell-Harris et al., 2024). None of these studies have so far involved pigmented genotypes, much less durum wheat ones.

In this framework, this study aimed to explore the effect of the biotic stress caused by *Fusarium graminearum* infection on phenylpropanoid biosynthetic pathway in durum wheat spikes. In order to highlight the alterations of phenylpropanoids and flavonoids due to the infection, especially for compounds scarcely present in wheat (such as anthocyanins), a genotype (Purple durum) in which these molecules are particularly accumulated was considered. Alterations in Purple durum were compared with those of two not-pigmented genotypes, chosen for their different susceptibility to FHB: Svevo (susceptible) and DBC-480 (resistant). Two time points were considered: an early stage (2 days post-infection, DPI), chosen because SAR activation is more evident at this stage, and a late stage (21 DPI), selected as optimal for studying pigmentation-related traits. Changes in the pathway were detected by (I) differential gene expression (by RT-qPCR) of key structural and regulatory genes; (II) targeted metabolomics, using HPLC/MS-MS for the quantification of 14 different phenylpropanoids present in the spikes in soluble or cell wall bound fractions; (III) total phenolic content assessed by Folin-Ciocolteu (F-C) assay; (IV) 2,2-Diphenyl-1-picrylhydrazyl (DPPH) scavenging assay to assess the antioxidant properties of the spike extracts.

2. Materials and methods

2.1. Plant material and growth condition

Three durum wheat genotypes (*Triticum turgidum* subsp. *durum*) were used in the present study. Svevo is a commercial early maturing cultivar with high protein content and yellow index, used as FHB susceptible control. Purple Durum is a pigmented durum wheat genotype (accession number NGB 6399), with purple grain pericarp, originally collected in Ethiopia and provided by Nordic Baltic Genebanks (GENBIS). The FHB-resistant durum wheat experimental line DBC-480, harboring the introgression of the resistant quantitative trait locus *Fhb1* from Sumai-3, was provided by IFA-Tulln (Prat et al. 2017). The experiment was carried out in a growth chamber equipped with white led light (Combo 600 W and Slim Natural Indoor bars, C-Led, Italy), controlled temperature and relative humidity. The kernels were germinated on paper soaked in sterile distilled water for 7 days at 20 °C with a 16 h photoperiod and then transferred to 9 × 9 cm pot filled with TYPical Brill soil. Plants were grown at 10 °C with an 8 h photoperiod for 2 weeks to break the dormancy and then each plant was transferred to a 2 L pot (12,8 × 12,8 × 20 cm), filled using the same soil, and plants were grown at 20 °C (±2 °C), 16 h photoperiod and 60% relative humidity until the end of the experiment. The plants were fertilized using calcium nitrate (15.5–0–0 + 26.5 CaO, Haifa) at every transplanting event and at heading using a micronutrient liquid fertilizer (NPK 4–7–7 + *B*+Cu+Fe+Mn+Zn, Flortis).

2.2. Fungal material and inoculum preparation

The highly virulent and DON-producing isolate of *F. graminearum* wild type 3824 was isolated for the first time by the University of Pisa (Tomassini et al. 2009). The inoculum was prepared following literature references (Francesconi and Balestra 2020). In brief, the isolate was cultured at 24 °C on Synthetic Nutrient Poor Agar (SNA) to obtain macroconidia. After 15 days on SNA, the conidia were scraped with a glass rod after pipetting 1 mL of sterile distilled water onto the surface of a Petri dish. The conidial suspension was recovered, and the concentration was adjusted to 1×10^6 conidia mL^{-1} using a Thoma Chamber (0.100 mm depth and 0.0025 mm^2). The inoculum was prepared in sterile distilled water supplemented with 0.05% (v/v) of Tween-20.

2.3. Experimental design, infection technique, disease evaluation and spike sampling

Plants were subjected to artificial inoculation at anthesis (Zadok stage 69) using a point inoculation technique. In brief, 10 µL of spore suspension were applied to the central spike floret of each plant (using a laboratory pipette), for the inoculated plants, while 10 µL of sterile distilled water supplemented with 0.05% (v/v) of Tween-20 were applied for mock plants. For each genotype, three replicates consisting of 10 plants each were considered for each treatment (inoculated and mock) using a completely randomized experimental design. The FHB disease severity (%) was determined by counting the number of bleached spikelets (number of infected spikelets on the total number of spikelets per spike) for each inoculated spike at 2 and 21 DPI (days post infection). At the same time points, three randomly chosen spikes were collected, suddenly frozen in liquid nitrogen and stored at −80 °C until RNA/metabolites extraction. Three biological replicates were considered for each experimental group.

2.4. RNA extraction, quality check, quantification and cDNA synthesis

Spikes were grinded to a fine powder using mortar and pestle in liquid nitrogen. The RNAzol RT reagent (Sigma-Aldrich) was used to extract pure total RNA from 50 mg of fresh plant tissue (Chomczynski et al. 2010). Briefly, 1 mL of RNAzol RT reagent and 400 µL of RNAase-free water were added to the sample. Sample and solution were shacked at 500 RPM for 15 min and then centrifuged 15 min at 13,000 g. The RNA-containing aqueous phase was precipitated with 1 mL isopropanol. The RNA pellet was washed with 75% ethanol and then resuspended in 50 µL of RNAase-free sterile deionized water. RNA purity was checked using a microvolume UV–Vis spectrophotometer (OPTIZEN NanoQ, KLAB, Republic of Korea) with A_{260}/A_{280} ratio of 1.7 to 2.1 and A_{260}/A_{230} of 1.6 to 2.3. RNA was quantified with a Qubit™ fluorometer 1.01 (Invitrogen) using the Qubit™ RNA BR Assay Kit (Thermo Fisher Scientific). The synthesis of cDNA was performed using 50 ng of RNA following the instructions provided by Xpert cDNA Synthesis Supermix with a gDNA eraser (GRiSP Research Solutions, Porto, Portugal) in a final volume of 20 µL. gDNA Contamination was checked through visualization on 1.5% agarose gel.

2.5. Primer design and relative gene expression

Starting from existing literature, mainly related to bread wheat (Ma et al. 2016; Jiang et al. 2018), the primer pairs for Real-Time qPCR were redesigned, adapted or verified on known sequences of durum wheat genome. Primer design was performed using the National Center for Biotechnology Information (NCBI) tool Primer-blast (https://blast.ncbi.nlm.nih.gov/Blast.cgi), using sequences obtained in Ensembl Plants (https://plants.ensembl.org/index.html) belonging to the INSDC Assembly GCA_900,231,445.1 (cv Svevo) (CNR). When annotation information was insufficient, sequences in NCBI (https://www.ncbi.nlm.nih.gov/) were considered. Primers were designed inside the exonic regions. The optimal annealing temperature was assessed by running a gradient PCR for each primer pair (range 59 °C – 63 °C). Primers used in this study are listed in Supplementary file S1. The relative expression levels of the target genes were calculated on the basis of the Ct values of the three technical replicates derived from three independent biological replicates for each wheat genotype a by the comparative C_T method (Schmittgen and Livak 2008), considering both relative expression of

ΔC_T, obtained by the following equation:

$$\text{Relative expression}_{\Delta Ct} = 2^{(-\Delta Ct)}$$

using *TaFNR, TaTUB* (Tenea et al. 2011), and *TaACT* (Tundo et al. 2016) as reference genes, and the relative expression normalized on the mock treatment (Bustin et al. 2009):

$$\text{Relative expression}_{\text{Mock normalization}} = 2^{(-\Delta\Delta Ct)}$$

The RT-qPCR was performed following the instructions provided by Rotor-Gene Q (Qiagen, Hilden, Germany) and Xpert Fast SYBR (uni) MasterMix (GRiSP Research Solutions, Porto, Portugal), in a final volume of 10 µL. The amplification conditions consisted of (i) an initial denaturation step of 10 min at 95 °C; (ii) 40 cycles of 5 s denaturation at 95 °C; (iii) 30 s of annealing at the temperature indicated in Supplementary file S1, and (iv) 20 s of elongation at 72 °C. A final melt cycle (72–95 °C) was performed to confirm the unicity of the amplicons. NTC controls were included and the amplification was considered negative when a value of Ct ≥ 38 was detected.

2.6. Extraction of soluble metabolites and cell wall bound metabolites

Extraction procedure was adapted from existing literature (Doppler et al. 2022; Wang et al. 2013). Two hundred mg of grinded spikes, stored at −80 °C, were freeze-dried and used for further extraction by adding 1 mL of a mixture of methanol and water (90:10) acidified with 5% formic acid. Samples were vortexed for 10 s, shaken for 10 min at 250 rpm, ultrasonicated for 5 min, and finally shaken for 5 min at 250 rpm. After centrifugation (5 min, 1300 rpm), the supernatant (extract I) was transferred to a new tube and the remaining pellet was used for a second extraction. After the second extraction, the supernatant (extract II) was pooled with the extract I, filtered (Choice™ PTFE Syringe Filters 0.22 µm x 13 mm, Thermo Scientific, Waltham, MA, USA) and used for HPLC-MS/MS analysis. The remaining pellet was employed for cell wall hydrolysis, that was carried out using 1 mL of NaOH 3 M under shaking conditions at room temperature for 2 h at 250 rpm. After this step, 100 µL of 25% HCl were added to adjust the pH to 1–1.5 units and samples were extracted using 500 µL of ethyl acetate by shaking 10 min at 250 rpm. After centrifugation (10 min, 1300 rpm) the ethyl acetate phase was transferred in a new tube. Ethyl acetate extraction was repeated twice and the collected and combined extracts were dried using a nitrogen evaporator. The residue was reconstituted with a solution of methanol: formic acid 80:20, filtered (0.2 µm) and used for the analysis. Soluble fraction (obtained by extraction using the mixture of methanol and water) and cell wall bound fraction (provided by hydrolysis) were analyzed separately.

2.7. Analytical determination of metabolites in durum wheat spike extracts

HPLC analyses were carried out using an HPLC 1260 Infinity II system (Agilent Technologies Italy S.p.A. Milan, Italy) coupled with QTRAP 5500 mass spectrometer (AB SCIEX S.r.l. Forster City, CA, USA) equipped with an ESI source, operating in MRM (multiple reaction monitoring) mode. The following phenolic acids and flavonoids were analyzed: caffeic acid, ferulic acid, gallic acid, *p*-coumaric acid, syringic acid, vanillic acid, 4-methoxyflavove, chlorogenic acid cyanidin 3-(6″ malonylglucoside), cyanidin 3-glucoside, delphinin 3-glucoside, kaempferol, oenin chloride (Malvidin-3-O-glucoside), quercetin. All the analytical specifications are reported in Supplementary material S2.

2.8. Folin-Ciocalteu (F-C) assay

A rapid, small-scale, high-throughput assay for approximating the total phenolic compounds on the basis of the improved Folin-Ciocalteu (F-C) method of Singleton and Rossi (Singleton and Joseph, 1965), using ferulic acid as a standard, was used, following literature references with minor modification (Ainsworth and Gillespie 2007; Schiavi et al. 2022). 100 µL of the extract used for metabolites quantification was used for the analysis. A 10-fold dilution of Folin-Ciocalteu reagent was made using deionized water and 750 µL of this dilution was added to the samples and incubated 10 min at room temperature. Then, 750 µL of a 2% sodium carbonate (Na_2CO_3) (CAS No: 497–19–8, Sigma-Aldrich) aqueous solution (w/v) was added and the mixture was incubated in the dark for 3 h. 200 µL of each sample were then transferred to a 96-well plate, considering 4 technical replicates for each experimental sample, and the absorbance was measured at 765 nm using a DR-200B Microplate reader (Diatek instruments). Final results were expressed as ferulic acid equivalent (FAE), related to the initial real sample weight, and using a ferulic acid (CAS No: 537–98–4, Sigma-Aldrich) calibration curve (ranging from 25 to 350 mg l^{-1} with an $R^2 = 0.9908$).

2.9. Determination of antioxidant capacity (DPPH)

The free radical scavenging capacity of each extract was determined by the use of the 2,2-Diphenyl-1-picrylhydrazyl (DPPH) radical, according to the method of (Dudonné et al. 2009) with few modifications. Briefly, a DPPH• solution in methanol (6×10^{-5} M) was prepared daily, and 1.5 mL of this solution was mixed with 50 µL of methanolic solutions of plant extracts. The samples were incubated for 20 min in the dark, and then dispensed in 96-well microplate (200 µL in each well, four technical replicates). The decrease in absorbance at 517 nm was measured (A_E) using a DR-200B Microplate reader (Diatek instruments). A blank sample containing 100 µL of methanol in the DPPH• solution was prepared daily, and its absorbance was measured (A_B) for each plate in 8 technical replicates. Radical scavenging activity was calculated using the following formula:

$$\%\text{inhibition DPPH} = [(A_B - A_E) / A_B] \times 100$$

where A_B is the absorbance of the blank sample, and A_E stands for the absorbance of the plant extract.

2.10. Data analysis

Kruskal-Wallis test and Dunn's post-hoc test were employed to evaluate the effect of genotypes on severity and relative gene expression, the effect of the infection on metabolites quantification, total phenolic content, and DPPH radical scavenging activity. Two level of significance ($p < 0.05$ and $p < 0.01$) was computed to assess the significance of the F values. Two-way PERMANOVA (with Bray–Curtis similarity index) was used to evaluate the combined effect of genotype and inoculation on metabolites composition of spike extracts. Linear correlation (Sperman's *rs* with Bonferroni correction) was employed to correlate metabolites quantification F-C and DPPH scavenging activity. Two heatmaps (one for each time point) were generated to represent the relative expression levels of wheat genes after the inoculations and analyzed by hierarchical clustering, where both rows and columns are clustered using correlation distance and average linkage. Summary statistics, normality test, Kruskal–Wallis test, Dunn's test of multiple comparisons, PERMANOVA and linear correlation were performed in PAST ver. 4.05 (University of Oslo) (Hammer and Harper 2005). ClustVis (Tartu, Estonia) web tool (https://biit.cs.ut.ee/clustvis/) was used for heatmap generation and hierarchical clustering (Metsalu and Vilo 2015). A summary pathway with considered metabolites and genes were built using PathVisio (Maastricht University, NL) a free open-source pathway analysis and drawing software (Kutmon et al. 2015).

3. Results

3.1. Disease severity

Plants were inoculated at anthesis and severity was evaluated at two different time points. As expected, the severity was very low at early stage, with no significant differences observed among genotypes (Purple durum, Svevo and DBC-480) (Fig. 1). At late stage of infection, the median severity of the resistant genotype DBC-480 was notably low (26.07%), showing high resistance to the infection. In contrast, Purple durum exhibited a median severity (83.56%) comparable to the susceptible genotype Svevo (100%), as displayed in Fig. 1 and in Supplementary file S3, in agreement with our previous study (Felici et al., 2024). Mock treated plants presented no visible symptoms.

3.2. In the early infection stage, all the considered genes were upregulated in the resistant control DBC-480

The expression of key genes involved in the phenylpropanoid and flavonoid pathways in durum wheat spikes was evaluated under artificial inoculation. *In silico* analysis revealed that only a few of the primer pairs available in the literature (designed for bread wheat) were suitable for RT-qPCR amplification in durum wheat. For this reason, five out of the seven target genes were redesigned (Supplementary file S1). The specificity and differentiation of the products were verified through analysis of amplicon melting curves at the end of RT-qPCR (Supplementary file S3).

As preliminary analysis, relative expression of the ΔC_T was considered as an assessment of differential gene regulation in comparison with housekeeping genes (Supplementary material S4). At early infection stage *PAL, DFR, F3H*, and *PPM1* showed a relative expression lower than 1-fold in all the considered genotypes, indicating an expression level lower that the reference genes, compatible with the expression of secondary metabolism related genes. For *C4H, CHS* and *COMT* only in infected DBC the relative expression was higher than 2-fold, while *COMT* was 1.88-fold more expressed that the reference genes in infected Svevo spikes', and 1.65-fold in healthy Svevo spikes'.

A graphical representation of the relative expression of the $\Delta\Delta C_T$ of the selected genes, normalized on mock treated samples, in the early infection stage (2 DPI) is shown in Fig. 2. *PAL* exhibited upregulation across all genotypes, with particularly notable increases in DBC-480 (71.87-fold) and Purple durum (15.01-fold). Similarly, *Fusarium* infection increased the expression level of *C4H* in DBC-480 (5.68-fold) and Purple durum (3.13-fold) compared to Svevo. *CHS* was upregulated in DBC-480 (2.70-fold) and slightly upregulated in Purple durum (1.45-fold), while in Svevo it showed a basal expression. *DFR* was upregulated in the resistant genotype (6.30-fold), and slightly upregulated in the pigmented genotype (1.49-fold), compared to the susceptible control that showed basal expression level (1.11-fold). *COMT* and *F3H* were upregulated in DBC-480 (3.80-fold and 3.32-fold, respectively), whereas no significant differences were observed in the other genotypes.

3.3. In the late infection stage PAL and C4H were upregulated in Svevo while CHS and PPM1 are upregulated in Purple Durum

Considering the relative expression of the ΔC_T at late infection stage (Supplementary material S4), for all genes the expression was generally higher than the early infection stage, suggesting an increased activation of the pathway at this time point. Some of the genes were particularly boosted compared to the housekeeping, such as expression of *COMT* in infected Purple durum (3.14-fold) and *F3H* in both infected and healthy DBC spikes showed relative expression of 5.13-fold and 6.79-fold respectively.

Normalizing the expression on mock treated plants, a clear change in the expression patterns among the different genotypes was evident in the late infection stage (21 DPI) compared to the early infection one, as shown in Fig. 2. *PAL* (38.40-fold) and *C4H* (57.47-fold) were strongly boosted in Svevo, compared to the 2 other genotypes. *CHS* was upregulated in Purple durum (4.14-fold) and Svevo (3.28-fold), whereas it was not differentially expressed in DBC-480 (0.92-fold). Interestingly, *PPM1* was boosted in Purple durum (6.19-fold) and Svevo (2.88-fold), compared to DBC-480 (1.04-fold), that showed a basal expression level. *COMT* and *F3H* were upregulated in Purple durum (4.79-fold and 1.49-fold, respectively), although these expression levels were not statistically different from those observed in the other two genotypes. *DFR* showed upregulation in DBC-480 (3.29-fold), in Svevo (2.68-fold), whereas no significant difference was observed in Purple durum (1.28-fold).

3.4. In the late infection stage soluble metabolites accumulation depends on both genotype and infection

Selected metabolites were extracted from spikes and quantified (using HPLC-MS/MS and reference standards), and expressed as ng g^{-1} of

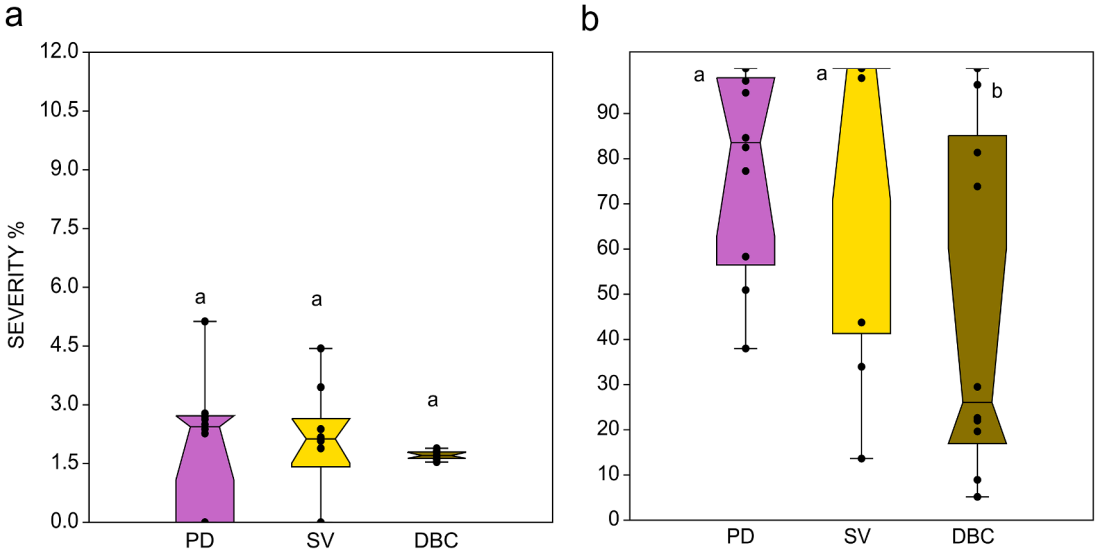

Fig. 1. Box plot of severity % at 2 DPI (a) and at 21 DPI (b), with $n = 10$. Different letters (a, b) into the subfigures refer to the statistical analysis performed using Kruskal-Wallis with the Dunn's test at a confidence level of 0.95 and $p < 0.05$. PD= Purple durum; SV= Svevo; DBC= DBC-480.

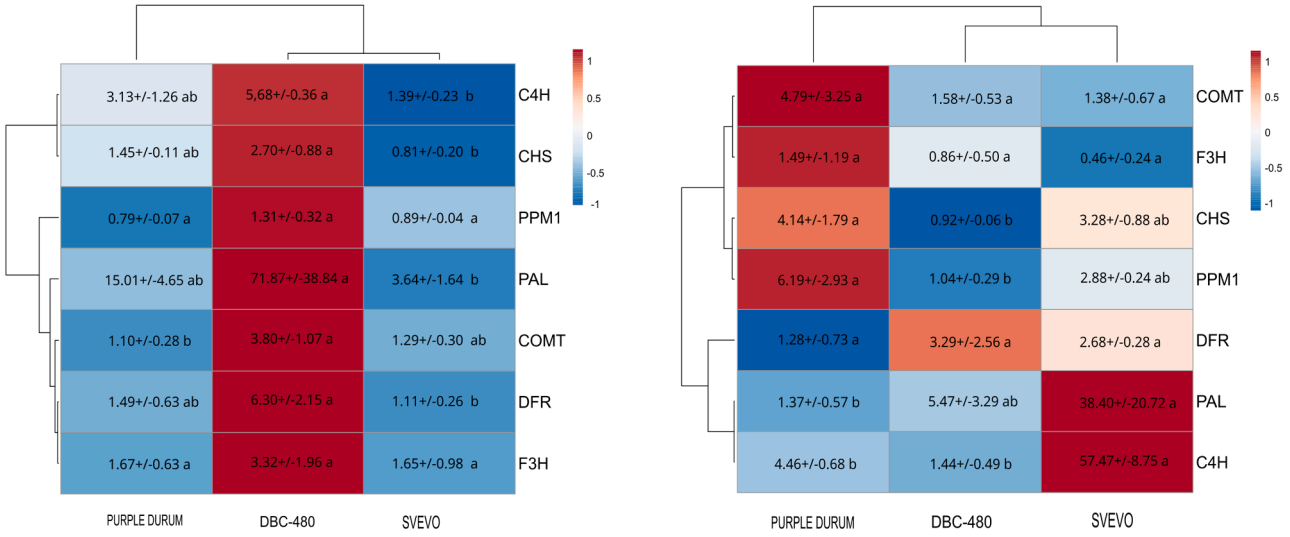

Fig. 2. Clustering analysis representing the relative expression of considered genes (rows) for each genotype (columns) due to *F. graminearum* infection, normalized on the un-infected (mock) control: (left) 2 DPI; (right) 21 DPI. Both rows and columns are clustered using correlation distance and average linkage. The heatmaps were constructed with the z-score (explained by the color legend at the right of the picture) by analyzing data with ClustVis software (Tartu, Estonia); numbers are the mean relative gene expression ± SE; letters refer to statistical difference (Kruskal-Wallis; Dunn's post-hoc) among genotypes for each gene.

starting biomass, in terms of soluble and cell wall bound fraction. The results obtained from the quantification of soluble metabolites are graphically displayed in Fig. 3a and 3b, while the data expressed in ng g^{-1} and the results of two-way PERMANOVA are shown in Supplementary file S5. At the early infection stage, the total amount of the considered metabolites stood below 900 ng g^{-1}. *p*-Coumaric acid was the most prevalent extracted compound. The two-way PERMANOVA analysis revealed that variability at the early infection stage depends exclusively on the genotype ($p < 0.01$). On the other hand, at 21 DPI, an increase in metabolite content was observed in infected Purple durum and Svevo compared to mock control plants (Fig. 3b). Indeed, in infected Purple durum and Svevo plants, the total amount of extracted metabolites was above 7000 ng g^{-1}, while in infected DBC-480, in mock DBC-480, Purple durum and Svevo plants this was below 2000 ng g^{-1}. Interestingly, a notable amount of cyanidin 3-(6″ malonylglucoside) (1878.88 ng g^{-1} infected; 586.17 ng g^{-1} mock) and Cyanidin 3-glucoside have been detected in Purple durum (670.92 ng g^{-1} infected; 138.31 ng g^{-1} mock), while vanillic acid was among the most abundant compounds detected in Purple durum and Svevo infected plants (829.53 ng g^{-1} Purple durum; 650.10 ng g^{-1} Svevo). The two-way PERMANOVA analysis revealed that variability at 21 DPI was dependent on the genotype and the infection ($p < 0.01$).

Quantification of selected cell wall bound metabolites is shown in Fig. 3c and 3d and in Supplementary files S4. Notably, all the samples, at early and late infection stages, were mainly composed of ferulic acid, *p*-coumaric acid, vanillic acid and syringic acid and the total amount of selected metabolites was above 16,000 ng g^{-1}. The two-way PERMANOVA analysis revealed that variability was independent from the genotype and the infection ($p > 0.05$).

3.5. *Fusarium infection affects the accumulation of the selected metabolites*

In order to focus on the infection effect, differences between the metabolite amounts in infected spikes (FG) and mock treated spikes were calculated for each considered metabolite (Table 1). Furthermore, statistical analysis was performed to compare FG-infected plants and mock treated plants (Kruskal-Wallis $p < 0.05$, indicated as "*" and bold font in the Table 1). At the early time point (2 DPI), the detection of metabolites in the soluble fraction of Svevo infected spikes revealed an increase in the accumulation of ferulic acid (+14.50%), a decrease in vanillic acid (−23.31%) and a surprising increase of cyanidin 3-(6″-malonylglucoside) (+252.46%) compared to mock treated plants. Detection of metabolites in the cell wall bound fraction of Svevo infected spikes showed a consistent increase of *p*-coumaric acid (+15.50%) and syringic acid (+45.43%) due to the infection. In DBC-480 infected spikes there was an increase of *p*-coumaric acid in the soluble fraction (+26.24%), while Purple durum infected spikes presented an increase in soluble quercetin and a decrease in bound quercetin (+98.75% in soluble fraction; −35.99% in cell wall bound fraction).At the late infection stage (21 DPI), alle three genotypes showed a significant increase in the accumulation of phenolic acids in the soluble fraction in the infected spikes compared to the mock treated ones. In all genotypes, a notable increase in *p*-coumaric acid (+189.64% DBC-480; +1202.41% Purple durum; +2706.82% Svevo) and vanillic acid (+44.51% DBC-480; +720.33% Purple durum; +1018.84% Svevo) was detected in soluble fraction, while an additional increase in ferulic acid was detected in Svevo and Purple durum soluble fraction (+569.64%; +880.29% respectively). An increase of soluble oenin (+83.76%) in infected spikes was statistically significant compared to the mock treated plants.

3.6. *Antioxidant activity of spike extracts is affected by the infection*

The antioxidant activity of the extracts obtained from the spikes (soluble fraction and cell wall bound fraction) were analyzed using the Folin-Ciocalteau assay (F-C) and the DPPH assay. F-C assay is an indirect estimation of the antioxidant potential of the extract, based on the assessment of the total amount of phenolic compounds in the samples, while the DPPH is a direct method based on the reactivity of 2,2-diphenyl-1-picrylhydrazyl, a free radical, which shows hydrogen acceptor ability towards antioxidants (Kurechi et al. 1980). F-C assay results were expressed as mg FAE/kg of starting biomass and showed in Fig. 4a-b-c-d. The infection increased the accumulation of soluble total phenolic content in Purple durum and Svevo at early infection stage (Fig. 4a), while at late infection stage only in Purple durum there were a statistically relevant increase (Fig. 4b). Cell wall bound total phenolic content at 2 DPI was not affected by the infection (Fig. 4c), while at 21 DPI DBC-480 and Purple durum displayed an increase in the infected plants (Fig. 4d). TPC (F-C assay) is higher in DBC-480 spike extract than Svevo spike extract, without *F. graminearum* infection (Fig.3a-d). These findings were partially confirmed by DPPH assay (Fig. 5a-b-c-d). At the early infection stage all the soluble extracts exhibited a DPPH radical

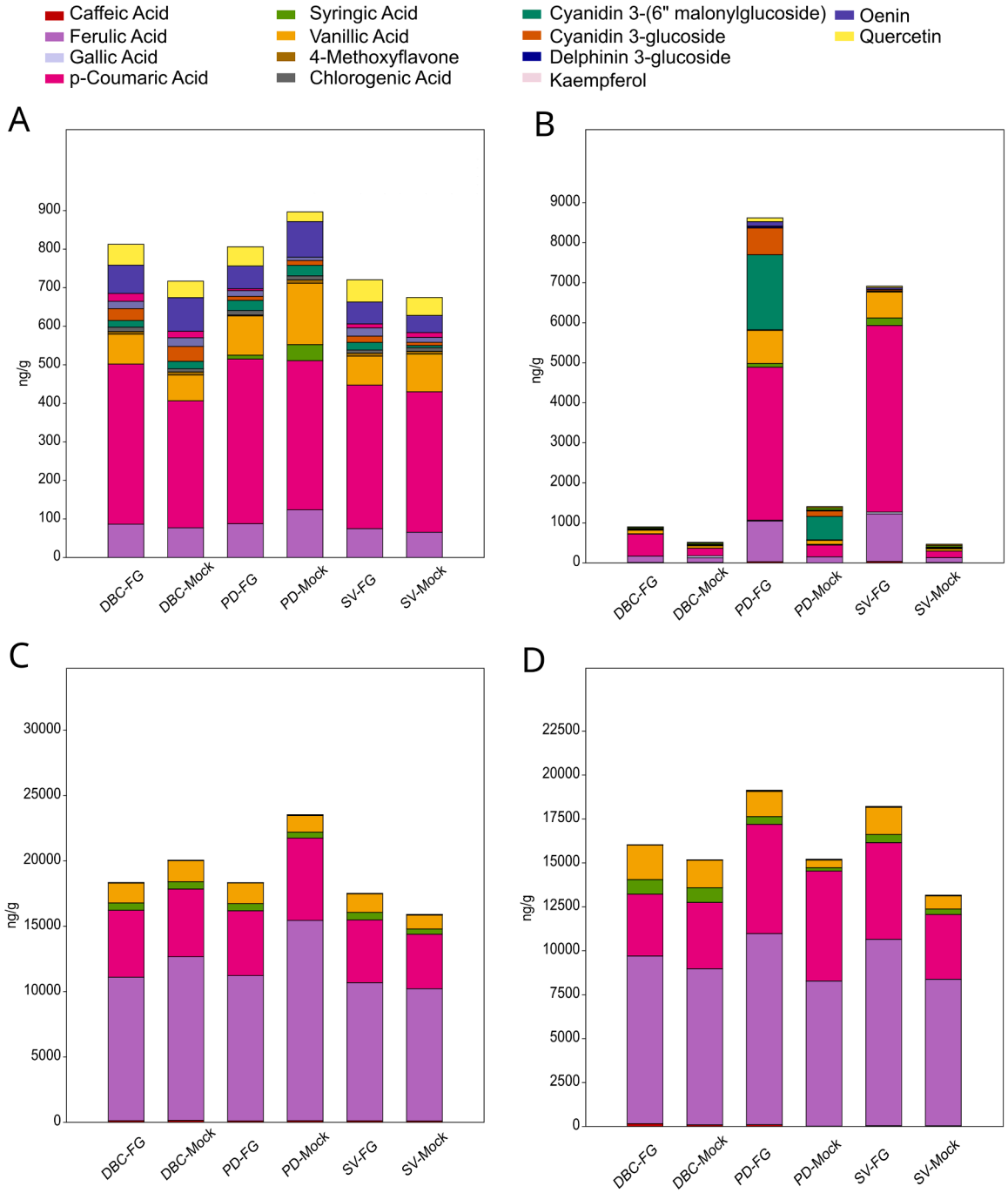

Fig. 3. Phenylpropanoids composition of DBC-480, Purple durum (PD) and Svevo (SV) *F. graminearum*-inoculated (FG) and Mock-treated spike extracts. (A) Soluble fraction at 2 DPI; (B) soluble fraction at 21 DPI; (C) cell wall bound fraction at 2 DPI; (D) cell wall bound fraction at 21 DPI.

scavenging activity ranging from 5% to 20% (Fig. 5a-b-c-d), highlighting that the infection did not have any significant effect on antioxidant activity (Fig. 5a). On the other hand, at 21 DPI, the DPPH radical scavenging activity of soluble fraction varied from 5% to 45% with the infection resulting in a notable increase in % DPPH inhibition across all genotypes (Fig. 5b). The infected spikes of pigmented genotype had the highest % inhibition of DPPH. Regarding the DPPH radical scavenging activities of the cell wall bound fraction, at 2 DPI, the infection led to an increase in the antioxidant activity in DBC-480 and Purple durum spikes' extracts (Fig. 5c). However, at 21 DPI, the antioxidant activity increased only in the infected resistant genotype (Fig. 5d).

3.7. Phenolic acids determine the antioxidant activity in soluble fraction but not in the cell wall bound fraction

A linear correlation (Sperman' *rs*) was computed in order to understand if antioxidant activity is more related to phenolic acids (PA), flavonoids (F) or to the total amount of the analyzed phenylpropanoids (PA+*F*). Data of F-C assay, % inhibition DPPH, analyzed phenolic acid (PA, sum of the concentration of caffeic acid, ferulic acid, gallic acid, *p*-coumaric acid, syringic acid and vanillic acid), analyzed flavonoids (F, sum of the concentration of 4-methoxyflavone, chlorogenic acid, cyanidin 3-(6″ malonylglucoside), cyanidol 3-glucoside, delphinin 3-glucoside, kaempferol, oenin, quercetin) and the total amount analyzed

Table 1
Differences (expressed in %) between *F. graminearum* infected plants (FG) and Mock treated plants for each metabolite quantified by HPLC/MS-MS. The data presented in the table (%) were obtained as follow: % = [(ng $g^{-1}_{(FG)}$–ng $g^{-1}_{(Mock)}$)/ng $g^{-1}_{(Mock)}$]x100. "*" Indicates that the difference (%) is statistically significant (Kruskal-Wallis $p < 0.05$).

		DBC 2 DPI	PD 2 DPI	SV 2 DPI	DBC 21 DPI	PD 21 DPI	SV 21 DPI
Caffeic Acid	Soluble frac.	0.00	0.00	0.00	−1.17	0.00	307.31
Caffeic Acid	Bound frac.	−12.55	−14.47	12.28	69.46	450.16	12.47
Ferulic Acid	Soluble frac.	11.82	−29.04	**14.50***	35.87	**569.64***	**880.29***
Ferulic Acid	Bound frac.	−12.36	−27.46	4.47	7.46	31.64	27.17
Gallic Acid	Soluble frac.	0.00	0.00	0.00	−100.00	0.00	0.00
Gallic Acid	Bound frac.	0.00	0.00	0.00	0.00	0.00	0.00
p-Coumaric Acid	Soluble frac.	**26.24***	10.34	2.18	**189.64***	**1202.41***	**2706.82***
p-Coumaric Acid	Bound frac.	−1.14	−21.27	**15.05***	−6.81	−0.76	49.29
Syringic Acid	Soluble frac.	0.00	−75.68	0.00	0.00	404.15	0.00
Syringic Acid	Bound frac.	0.14	19.69	**45.43***	−1.37	140.31	48.41
Vanillic Acid	Soluble frac.	15.74	−36.01	**−23.31***	**44.91***	**720.33***	**1018.84***
Vanillic Acid	Bound frac.	−5.39	25.03	32.31	25.89	233.13	106.67
4-Methoxyflavone	Soluble frac.	−17.37	−73.66	6.24	19.04	46.74	18.21
4-Methoxyflavone	Bound frac.	−18.61	−38.41	5.09	−2.87	43.93	55.80
Chlorogenic Acid	Soluble frac.	39.25	6.00	−14.42	−75.27	81.74	−21.05
Chlorogenic Acid	Bound frac.	−12.10	−47.43	−12.22	−28.70	−21.89	36.00
Cyanidin 3-(6″ malonylglucoside)	Soluble frac.	−10.91	−1.53	**252.46***	−6.16	219.51	−15.38
Cyanidin 3-(6″ malonylglucoside)	Bound frac.	−17.86	−3.54	3.42	3.49	44.99	0.00
Cyanidin 3-glucoside	Soluble frac.	−19.61	−17.87	101.39	207.48	385.09	392.66
Cyanidin 3-glucoside	Bound frac.	−7.55	−100.00	−100.00	0.00	40.28	−100.00
Delphinin 3-glucoside	Soluble frac.	−16.64	68.87	65.24	−11.34	123.67	11.30
Delphinin 3-glucoside	Bound frac.	0.00	−69.66	−43.57	−100.00	109.12	−100.00
Kaempferol	Soluble frac.	22.10	0.00	−17.66	0.00	147.27	−100.00
Kaempferol	Bound frac.	0.00	−68.09	43.39	−39.43	−5.69	29.58
Oenin Chloride	Soluble frac.	−15.94	−35.95	28.71	−15.47	**83.76***	24.78
Oenin Chloride	Bound frac.	0.00	−100.00	4.27	0.00	0.93	0.00
Quercetin	Soluble frac.	26.50	**98.75***	23.27	−67.36	228.26	5.10
Quercetin	Bound frac.	−8.57	**−35.99***	−0.86	−68.37	52.44	50.41

phenylpropanoids (PA+*F*) were used to run the linear correlation (Table 2 and Table 3). As displayed in table 2, in the spike soluble fraction the DPPH scavenging activity correlate with phenolic acid content ($rs = 0.5262$) and total phenylpropanoids ($rs = 0.6216$), while the F-C correlate with flavonoids content ($rs = 0.4720$) and there is no correlation DPPH-F-C. In cell wall bound fraction (Table 3) total phenylpronoids (PA+*F*) are strongly correlated with PA ($rs = 0.9997$), F-C correlate with PA content ($rs = 0.7750$) and there is a correlation DPPH-F-C ($rs = 0.5926$).

4. Discussion

Phenylpropanoids have several biochemical properties, but probably the most relevant feature is their antioxidant activity, which means their ability to inhibit (reduce) all molecules having high Ox/Red potential (Brainina et al., 2019). Our results showed that the *F. graminearum* infection influenced DPPH scavenging activity of spikes and grains (Figs. 4 and 5), and it could be influenced by phenolic acids or by flavonoids in the soluble fraction, while the considered metabolites did not explain the antioxidant activity in the cell wall bound fraction. In accordance with Wiwart et al. (2024), our results suggest that in durum wheat grains antioxidant activity is a complex trait which may depend on the concurrent accumulation of different groups of metabolites, rather than a single one or a single class. To understand the influence of *Fusarium graminearum* infection on the phenylpropanoid pathway at early (2 DPI) and late (21 DPI) infection stage, in this study 14 key metabolites (hydroxybenzoic acids, hydroxycinnamic acids and flavonoids) were quantified by HPLC-MS/MS and, at the same time, the expression of structural genes encoding PAL, C4H, CHS, F3H, DFR, and COMT, and the transcription factor Ppm1 were analyzed in durum wheat spikes using qRT-PCR, considering three genotypes differing in FHB resistance and grains pigmentation. The examined pathway is summarized in Fig. 6.

The starting point of the pathway is the conversion of phenylalanine into *t*-cinnamic acid through PAL enzyme (Fig. 6). According to our results, at the early infection stage, *PAL* is upregulated in all considered genotypes, with a notable boost in DBC-480, which harbors the QTL *Fhb1* from Sumai-3, conferring Type II resistance (resistance to spread along the spike) (Prat et al. 2017). These findings are consistent with several other studies. Indeed, *PAL* up-regulation induced by *Fusarium graminearum* has been previously reported in Type II resistant cv. Sumai-3 (Golkari et al. 2007) and derived line CM82036 in association with the 3BS QTL (Steiner et al. 2009) or other QTLs (Kage et al. 2018; Dhokane et al. 2016). Moreover, different studies suggested that plants synthesize salicylic acid, from cinnamate produced by PAL (Huang et al. 2010), activating the systemic acquired resistance (SAR) (Zhong et al. 2021; Sorahinobar et al. 2016; Francesconi et al. 2020). Notably, the differential expression of *PAL* firstly occurs before 2 DPI (Wu et al. 2022). The strong activation of *PAL* and *C4H* genes in the late infection stage (21 DPI) in Svevo is interesting. Other authors (Li et al. 2020b) found that, in bread wheat subjected to abiotic stress (drought stress), the expression of *PAL, C4H*, and *4CL* genes reached a high level between 15 DAA (day post anthesis) and 25 DAA. The upregulation of *PAL* and *C4H* during fungal infection at 21 DPI may suggest a late activation of phenylpropanoid pathway in the susceptible genotypes, insufficient to counteract *F. graminearum* action. C4H (cinnamate 4-hydroxylase) is a class II monooxygenase, which hydroxylates cinnamic acid to produce *p*-coumaric acid (Zhang et al. 2020). *p*-Coumaric acid serves as a precursor of a myriad of organic compounds essential for plant metabolism, structure, development, and defense, including stilbenes, chalcones, flavonoids, hydroxycinnamates, and lignin (Zhang et al. 2020). Together with ferulic acid, *p*-coumaric acid is an essential component of commelinid monocots secondary cell wall, where these two hydroxycinnamic acids are esterified with arabinoxylans, forming a complex matrix of various polysaccharides, proteins and lignin (Saulnier et al. 2012). The plant cell wall is one of the constitutive barriers that pathogens need to overcome to colonize plant tissues (Miedes et al. 2014). Indeed, in this study, the cell wall bound phenylpropanoid fraction from wheat spikes was mainly represented by ferulic acid and *p*-coumaric acid (Fig. 2c-d), but their concentration remained invariable between infected and mock treated plants at both time points and in all considered genotypes. This is in agreement with other studies, which identified ferulic acid and

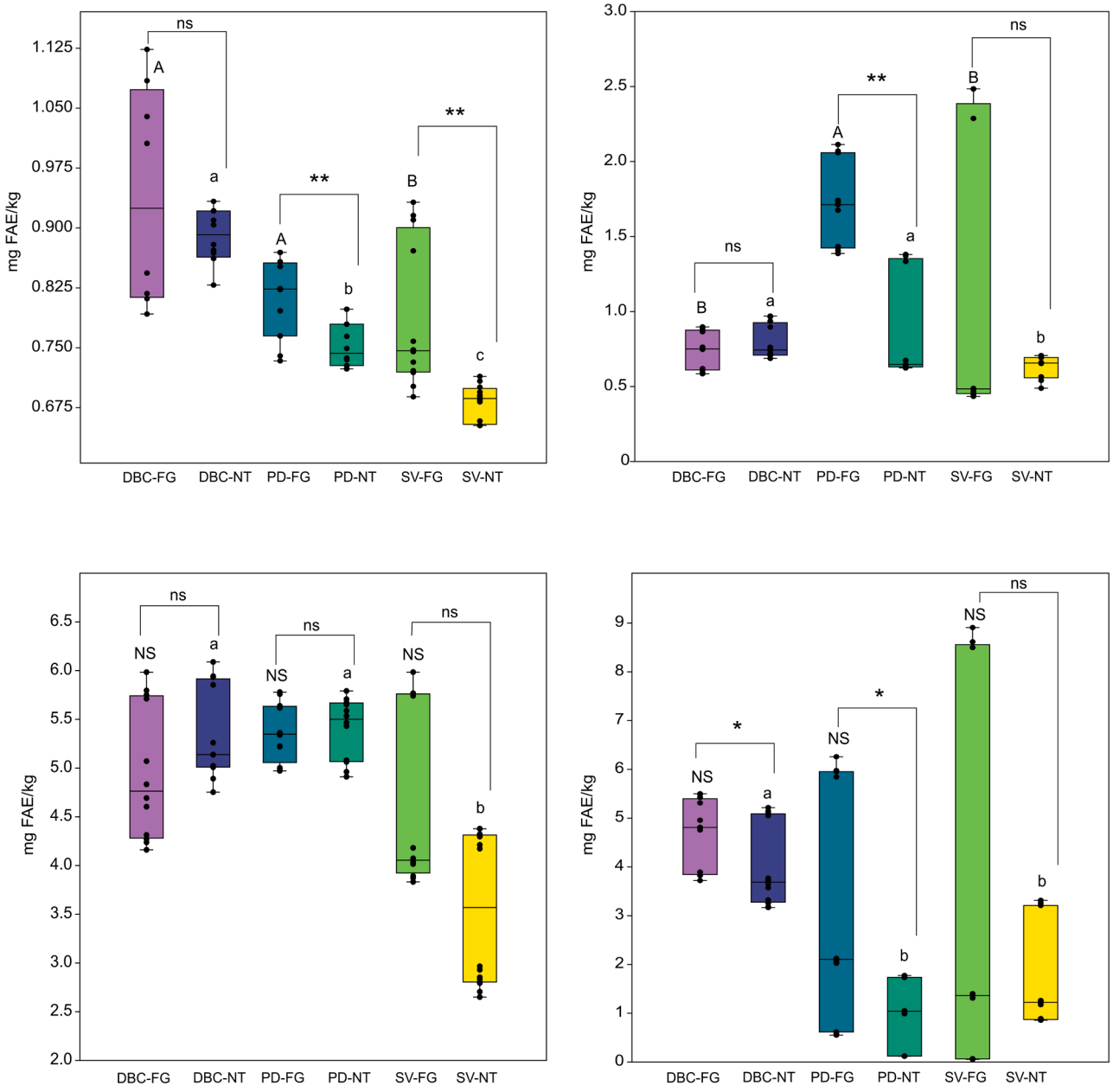

Fig. 4. Results of F-C assay of plant extracts, related to: (a) soluble fraction at 2 DPI; (b) soluble fraction at 21 DPI; (c) cell wall bound fraction at 2 DPI; (d) cell wall bound fraction at 21 DPI. Data were analyzed by Kruskal-Wallis test. Different letters indicate differences for $p < 0.05$ according to the Dunn's test. Upper case letters refer to statistical analysis of F-C in infected plant while lower case letters refer statistical analysis of F-C in mock treated plants. Statistical analysis between FG-infected spikes and mock treated ones (here indicated as "NT") were computed and the symbol "**" indicate significant differences at $p < 0.01$. "NS" or "ns" mean not significant difference.

p-coumaric acid as constitutive resistant related compounds (Gunnaiah and Kushalappa 2014; Bollina et al. 2011). This means that they are related to resistance (due to their involvement in cell wall thickening), but are not induced by the infection. Nevertheless, according to our results obtained at the late time point (21 DPI), there is an increase in the soluble fraction of ferulic acid, *p*-coumaric acid and vanillic acid in all the considered genotypes. These findings may suggest that the increase of these phenolic compounds is the result of a catabolic process rather than a metabolic one. Indeed, during the infection, *Fusarium* spp. can produce different cell wall degrading enzymes (CWDEs) to overcome the cell wall barrier, especially pectin degrading enzymes, such as xylanases (Kikot et al. 2009; Mandalà et al. 2021). Xylanases may degrade the link between arabinoxylans and phenolic acids, resulting in their release into the soluble fraction (Moreira and Filho 2016). Another important constituent of secondary cell wall is lignin. Lignin is a polymerized network of cinnamyl alcohols in plant cell walls that forms a network with the hemicelluloses, surrounding the cellulose microfibrils. Lignin biosynthesis occurs through the action of different enzymes (Goujon et al. 2003). Among them, *COMT* (caffeic acid O-methyltransferase) resulted upregulated in the present study in the resistant genotype at the early infection stage. This is in agreement with other studies, where early *COMT* overexpression increased biotic and abiotic stress tolerance (Bhuiyan et al. 2007; Yang et al. 2019; Gunnaiah et al. 2012). On the other hand, the differential expression of *COMT* at the late infection stage was not statistically different among the genotypes, and vanillic acid, a lignin-derived monomer, increased into the soluble fraction in all the genotypes. These results may indicate a late microbial depolymerization of lignin (Wang et al. 2018).

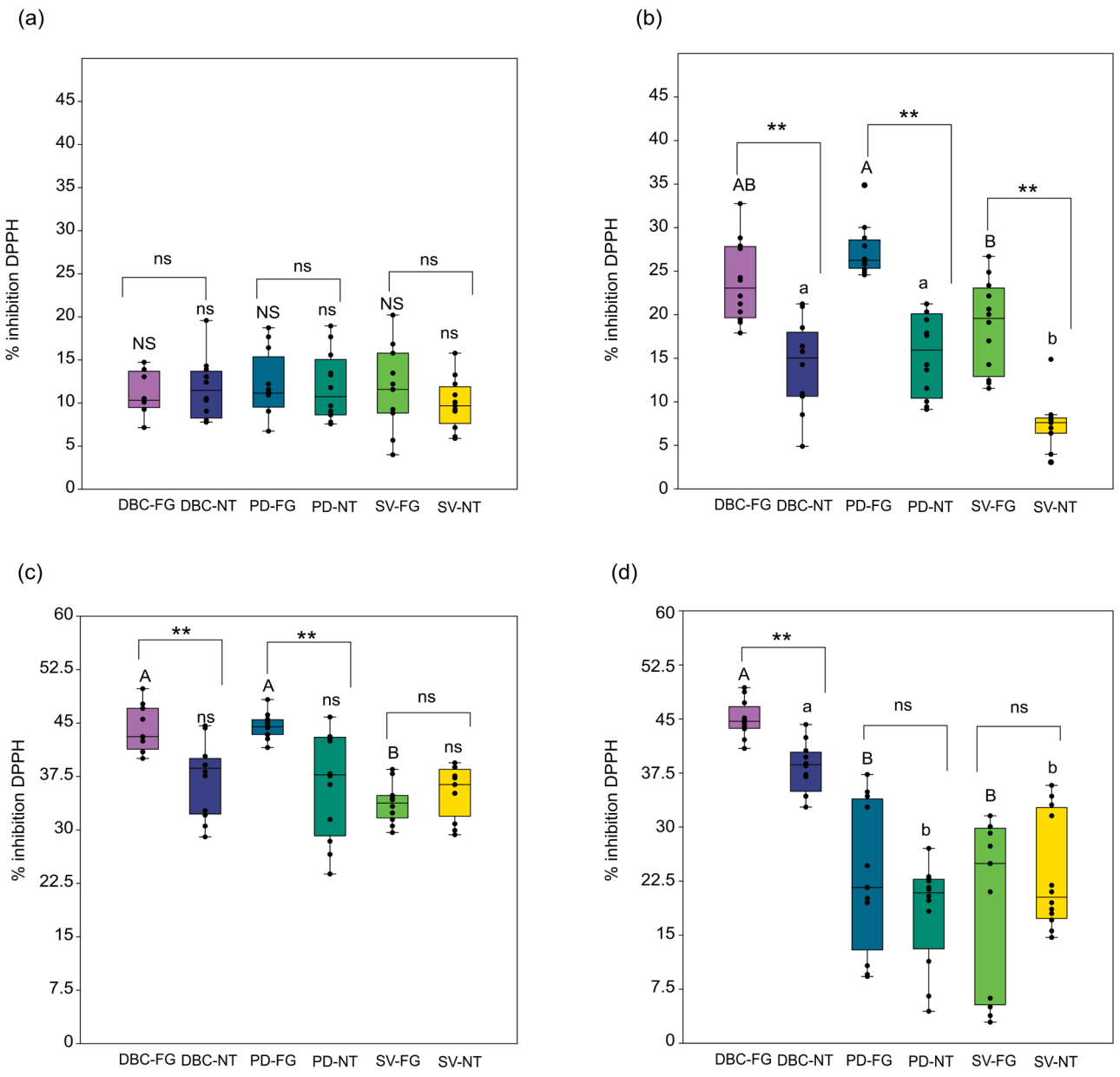

Fig. 5. DPPH scavenging activity of plant extracts, related to: (a) soluble fraction at 2 DPI; (b) soluble fraction at 21 DPI; (c) cell wall bound fraction at 2 DPI; (d) cell wall bound fraction at 21 DPI. Data were analyzed by Kruskal-Wallis test. Different letters indicate differences for $p < 0.05$ according to the Dunn's test. Upper case letters refer to statistical analysis of DPPH scavenging in infected plant while lower case letters refer statistical analysis of DPPH scavenging in mock treated plants. Statistical analysis between FG-infected spikes and mock treated ones (here indicated as "NT") were computed and the symbol "**" indicate significant differences at $p < 0.01$. "NS" or "ns" mean not significant difference.

Table 2
Sperman'*rs* coefficient related to soluble fraction. The symbols "*" and "**" indicate significant differences at $p < 0.05$ and $p < 0.01$, respectively. F-C = Folin-Ciocalteau assay.

SOLUBLE	Phenolic acids (PA)	Flavonoids (F)	Phenylpropanoids (PA+*F*)	F-C	% Inhibition DPPH
Phenolic acids (PA)	1				
Flavonoids (F)	0.16371	1			
Phenylpropanoids (PA+*F*)	0.78919**	0.5184**	1		
F-C	0.43221	0.47199*	0.36134	1	
% Inhibition DPPH	0.5562**	0.11401	0.62161**	0.40619	1

A second branch of the phenylpropanoids pathway leads to the biosynthesis of flavonoids (Fig. 6). Among the key enzymes involved in the flavonoids biosynthetic pathway, there are chalcone synthase (CHS), flavone 3-hydroxylase (F3H) and dihydroflavonol 4-reductase (DFR). According to our results, the genotype affects the differential expression of *CHS* at both considered time points. At the early time point, *CHS* was upregulated in DBC-480 compared to Svevo, while the opposite occurred at the late time point, when it was particularly upregulated in

Table 3
Sperman'*rs* coefficient related to cell wall bound fraction. The symbols "*" and "**" indicate significant differences at $p < 0.05$ and $p < 0.01$, respectively. F-C = Folin-Ciocalteau assay.

BOUND	Phenolic acids (PA)	Flavonoids (F)	Phenylpropanoids (PA+*F*)	F-C	% Inhibition DPPH
Phenolic acids (PA)	1				
Flavonoids (F)	0.26847	1			
Phenylpropanoids (PA+*F*)	0.99974**	0.27284	1		
F-C	0.77503**	−0.037323	0.77426**	1	
% Inhibition DPPH	0.30068	−0.4034	0.29811	0.59261**	1

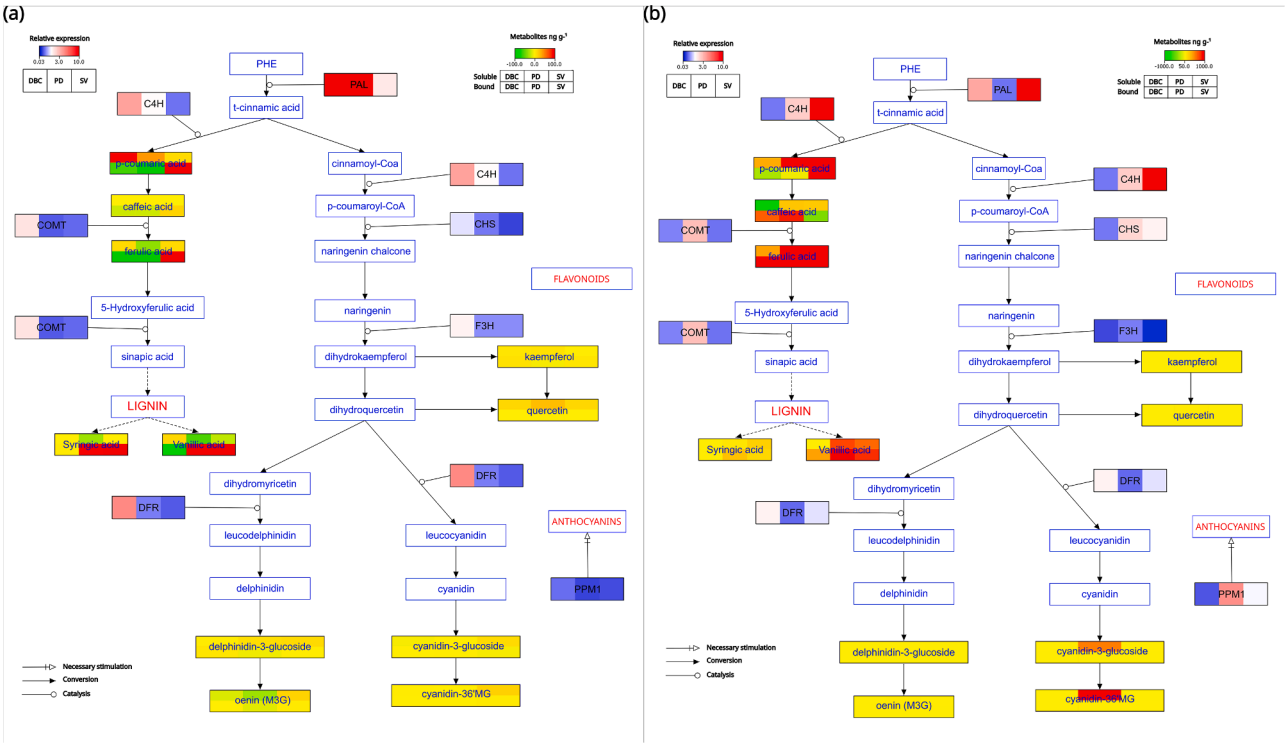

Fig. 6. Simplified phenylpropanoids pathway, indicating (by heatmaps) the metabolites increase or reduction due to infection and the relative expression of the coding genes or transcription factor analyzed in this study and presented in Fig. 1 and Table 1. Only the more interesting metabolites are displayed. Left pathway (a) refer to early infection stage, while right pathway (b) is related to late infection stage. PHE = phenylalanine; *PAL* = phenylalanine ammonia lyase; *C4H* = cinnamate 4-hydroxilase; *COMT* = Caffeic acid O-methyltransferase; *CHS* = chalcone synthase; *F3H* = flavone 3-hydroxylase; *DFR* = dihydroflavonol reductase; *Ppm1* = Purple pericarp MYB1; M3G = malvidin 3-O-glucoside; DBC = DBC-480; PD = purple durum; SV = Svevo.

Purple durum too. These results corroborate the outcomes of different authors who found that chalcone synthase family genes regulate the early response (1–4 DPI) against fungal pathogens (Li et al. 2023b; Ahmad et al. 2023). Li et al. (2020b) found a late upregulation of *CHS* in wheat spikes (15–20 DPI) under drought stress, but few authors analyzed the role of *CHS* gene family in response to stress at late stage, so far. While *CHS* seams to play a crucial role in stress response, *F3H* appears less insightful. In this study, at the early time point, *F3H* is upregulated in DBC-480, similar to the other considered genes, while at the late infection stage, it is downregulated in Svevo and DBC-480 and upregulated in Purple durum, but the effect of the genotype was not significant in both time points. Consistently with these findings, other authors found that *F3H* is downregulated in bread wheat under abiotic stresses, both at early (3–6 DAA) and late (20–25 DAA) time points (Li et al. 2023a; Li et al. 2020b). The current investigation also found that there was a slight increase in quercetin accumulation in the soluble fraction of Purple durum spikes and a slight reduction of quercetin in cell wall bound fraction. Quercetin in wheat could be present in both the soluble fraction and bound to the cell wall, where its glycosylated forms were recognized as a constitutive resistance related metabolite against FHB (Gunnaiah and Kushalappa 2014). Quercetin is known for its antifungal activity (Lalak-Kańczugowska et al. 2023) and recently it was employed as a synthetic elicitor to stimulate tomato response against Fusarium wilt (Hassan et al. 2023). The fact that the increase of quercetin in the soluble fraction occurs only in the pigmented genotype may be related to a slight early activation of flavonoids biosynthetic pathway, most likely related to the regulation of other genes not included in this study (such as chalcone isomerase, *CHI,* or flavonol synthase, *FLS*). The flavonoid pathway eventually continues through the biosynthesis of anthocyanins (Li and Ahammed 2023). The synthesis of these water-soluble plant pigments starts with the reduction of dihydroflavanols to leucoanthocyanins by dihydroflavonol 4-reductase (DFR). In this study, *DFR* was boosted in the resistant genotype at the early infection stage, while, in other studies, bread wheat under abiotic stresses showed a constitutive expression of this gene (Li et al. 2020b; Li et al. 2023a). The presence of anthocyanins in the yellow-pigmented genotype Svevo may appear surprising. Nevertheless, other authors have already identified cyanidin-3-glucoside and anthocyanidin in soluble and bound extracts of durum wheat Svevo grains (Dinelli et al. 2009). The slight increase of cyanidin 3-(6″ malonylglucoside) in Svevo after 2 days post infection can hardly be related to the regulation of *DFR* (which had basal expression in Svevo in this study) and it is most likely

related to the regulation of other genes not included in this study. At the late infection stage, *DFR* is up-regulated in DBC-480 and Svevo and slightly upregulated in Purple durum, but the effect of the genotype was not meaningful. This finding is partially in contrast with Li et al. (2020a) who found that the structural and regulatory genes involved in anthocyanin biosynthesis in a purple bread wheat cultivar under drought stress (15 DAA and 24 h post-stress induction) were downregulated, except for *TaDFR* that was upregulated (Li et al. 2020a). Interestingly, in this study, at the late infection stage, the transcription factor *Ppm1* was boosted in the pigmented genotype due to *F. graminearum* infection. The anthocyanin biosynthesis pathway is regulated by the MYB-bHLH-WD40 ternary complex (MBW) (Patra et al. 2013; Li and Ahammed 2023). Jiang et al. (2018) revealed that in bread wheat, the transcription factors MYB, located in the chromosome 7D (TaPpm1; 7D), and MYC, located in the chromosome 2A (TaPpb1; 2A), co-regulate anthocyanin production in the purple pericarp. Sharma et al. (2022) showed that pericarp-associated grain color is linked to abiotic stresses like temperature, drought, and UV irradiation. Li et al. (2020a) found that drought stress upregulates TaMYB-4B1 at 15 DAA and 24 h post-stress induction. To the best of our knowledge, this is the first report of a differential expression of *Ppm1* influenced by biotic stress in durum wheat. In the present study, we observed in Purple durum an increase in the soluble fraction at 21 DPI of cyanidin 3-(6″ malonylglucoside), cyanidin 3-glucoside and oenin (malvidin 3-O-glucoside), but only differences related to the latter one were statistically significant. This discrepancy may be due to the infection which, at the late stage, can widely compromise the spikes leading to a high variability in their composition and a strong degradation of some compounds, as the anthocyanins (Enaru et al. 2021). Moreover, *Ppm1* is grain-specific (Jiang et al. 2018), but Purple durum can accumulate pigments in other parts of the spike, like the glumes (Supplementary material S3) and in the present study the whole spike was considered. Thus, *Ppm1* may not explain the whole variability in anthocyanins accumulation of the samples.

5. Conclusion

Differential gene expression patterns were observed in the phenylpropanoids and flavonoid pathway genes across genotypes and infection stages. The genotype DBC-480 showed upregulation of several key genes involved in the phenylpropanoids pathway, particularly *PAL, C4H* and *DFR*, suggesting a potential involvement of these genes in the defense response. However, this upregulation was not accompanied by a parallel accumulation of metabolites, suggesting that the considered phenylpropanoids are not part of inducible defenses, but rather of the constitutive ones, as highlighted in the discussion. Notably, there was a substantial increase in metabolite content in infected Purple durum and Svevo compared to mock control plants with *Fusarium* infection affecting the accumulation of some metabolites, particularly phenolic acids, in both soluble and cell wall bound fractions. This may suggest that these metabolites are not enough to confer resistance to FHB, because they were induced only in the two susceptible genotypes. The infection led to notable changes in metabolite composition, indicating a dynamic interaction between the pathogen and the host plant and suggesting a genotype-dependent response to infection. In particular this study allowed to evaluate the modification of plant cell wall and of flavonoids composition, such as the anthocyanins, poorly investigated in durum wheat. The soluble fraction exhibited increased antioxidant activity in response to infection, indicating a potential defense mechanism against oxidative stress induced by *Fusarium* infection. However this mechanism is shared among the genotypes, suggesting a lack of direct correlation with the resistance. In conclusion, this study highlights a dynamic interplay between genotype, gene expression, metabolite accumulation, and antioxidant activity in durum wheat spikes in response to F. *graminearum* infection. Nevertheless, the main limitation of this study is the restricted number of genes and metabolites evaluated. Considering these results, future studies should examine phenylpropanoid and flavonoid pathway in a more comprehensive way, such as using omics sciences. These findings contribute to the understanding of host-pathogen interactions for future breeding programs focused on improving FHB resistance in durum wheat varieties.

Funding

This research was supported by the project Valorizzazione Multifunzionale di Frumenti Pigmentati per la realizzazione di Alimenti Funzionali e di NanoAgrofarmaci Green per la Protezione del Frumento acronym MULTIFRU funded by POR FESR Lazio 2014–2020 action 1.2.1 and by Departments of Excellence MUR Law 232/2016, and the research was carried out in the framework of the National program for "Departments of Excellence 2023–2027″ of MUR (DiVerSo Project) at DAFNE, University of Tuscia.

CRediT authorship contribution statement

Linda Felici: Writing – original draft, Visualization, Validation, Methodology, Investigation, Formal analysis, Data curation, Conceptualization. **Federica Castellani:** Methodology, Formal analysis, Data curation. **Sara Francesconi:** Writing – review & editing, Supervision. **Matteo Vitali:** Writing – review & editing, Supervision. **Francesco Sestili:** Writing – review & editing, Supervision, Project administration, Funding acquisition. **Giorgio Mariano Balestra:** Writing – review & editing, Supervision, Project administration, Funding acquisition.

Declaration of competing interest

The authors declare that they have no known competing financial interests or personal relationships that could have appeared to influence the work reported in this paper.

Data availability

Data will be made available on request.

Acknowledgements

The authors gratefully acknowledge Barbara Steiner and Hermann Bürstmayr (Department of Agrobiotechnology Tulln, University of Natural Resources and Life Sciences Vienna - BOKU) for kindly providing DBC-480 seeds to perform the experiments. The authors wish also to thank the Nordic Genetic Genebanks (GENBIS) for providing the seeds of the Purple Durum.

Supplementary materials

Supplementary material associated with this article can be found, in the online version, at doi:10.1016/j.stress.2024.100603.

References

Abdel-Aal, El-Sayed M., Rabalski, Iwona, 2008. Bioactive compounds and their antioxidant capacity in selected primitive and modern wheat species. Open Agric. J. 2 (1), 7–14. https://doi.org/10.2174/1874331500802010007.

Ahmad, Sheraz, Ali, Saqib, Shah, Amir Zaman, Khan, Ayesha, Faria, Sundas, 2023. Chalcone Synthase (*CHS*) Family Genes Regulate the Growth and Response of Cucumber (*Cucumis Sativus* L.) to Botrytis Cinerea and Abiotic Stresses. Plant Stress 8 (April), 100159. https://doi.org/10.1016/j.stress.2023.100159.

Ainsworth, E.A., Gillespie, K.M., 2007. Estimation of total phenolic content and other oxidation substrates in plant tissues using Folin-Ciocalteu reagent. Nat. Protoc. 2 (4), 875–877. https://doi.org/10.1038/nprot.2007.102.

An, C., Mou, Z., 2011. Salicylic Acid and its Function in Plant ImmunityF. J. Integr. Plant Biol. 53 (6), 412–428. https://doi.org/10.1111/j.1744-7909.2011.01043.x.

Aristimuño Ficoseco, M.E., Vattuone, M.A., Audenaert, K., Catalán, C.A.N., Sampietro, D. A, 2014. Antifungal and antimycotoxigenic metabolites in Anacardiaceae species from northwest Argentina: isolation, identification and potential for control of

Fusarium species. J. Appl. Microbiol. 116 (5), 1262–1273. https://doi.org/10.1111/jam.12436.
Atanasova-Penichon, V., Barreau, C., Richard-Forget, F, 2016. Antioxidant secondary metabolites in cereals: potential involvement in resistance to Fusarium and mycotoxin accumulation. Front. Microbiol. 7 (APR), 1–16. https://doi.org/10.3389/fmicb.2016.00566.
Belščak-Cvitanović, Ana, Durgo, Ksenija, Huđek, Ana, Bačun-Družina, Višnja, Komes, Draženka, 2018. Overview of polyphenols and their properties. In: Charis, M B T (Ed.), Polyphenols: Properties, Recovery, and Applications. Woodhead Publishing, pp. 3–44. https://doi.org/10.1016/B978-0-12-813572-3.00001-4 edited by Polyphenols: Properties Galanakis Recovery, and Applications.
Bhuiyan, Nazmul H, Liu, Weiping, Liu, Guosheng, Selvaraj, Gopalan, Wei, Yangdou, King, John, 2007. Transcriptional Regulation of Genes Involved in the Pathways of Biosynthesis and Supply of Methyl Units in Response to Powdery Mildew Attack and Abiotic Stresses in Wheat. Plant Mol. Biol. 64 (3), 305–318. https://doi.org/10.1007/s11103-007-9155-x.
Böhmdorfer, Stefan, Oberlerchner, Josua Timotheus, Fuchs, Christina, Rosenau, Thomas, Grausgruber, Heinrich, 2018. Profiling and quantification of grain anthocyanins in purple pericarp×blue aleurone wheat crosses by high-performance thin-layer chromatography and densitometry. Plant Methods 14 (1), 1–16. https://doi.org/10.1186/s13007-018-0296-5.
Bollina, Venkatesh, Kushalappa, A.C., Choo, Thin M., Dion, Yves, Rioux, Sylvie, 2011. Identification of metabolites related to mechanisms of resistance in barley against *fusarium graminearum*, based on mass spectrometry. Plant Mol. Biol. 77 (4–5), 355–370. https://doi.org/10.1007/s11103-011-9815-8.
Boukid, Fatma, 2021. Cereal-derived foodstuffs from north african-mediterranean: from tradition to innovation. In: Boukid, Fatma (Ed.), Cereal-Based Foodstuffs: The Backbone of Mediterranean Cuisine. Springer International Publishing, Cham, pp. 117–150. https://doi.org/10.1007/978-3-030-69228-5_5 edited by.
Boutigny, A., Barreau, C., Richard-forget, F, 2010. *Natural phenolic acids from wheat bran inhibit Fusarium culmorum trichothecene biosynthesis* in vitro *by repressing Tri gene expression* 275–286. https://doi.org/10.1007/s10658-010-9592-2.
Boutigny, A.-L., Barreau, C., Atanasova-Penichon, V., Verdal-Bonnin, M.-N., Pinson-Gadais, L., Richard-Forget, F, 2009. Ferulic acid, an efficient inhibitor of type B trichothecene biosynthesis and Tri gene expression in Fusarium liquid cultures. Mycol. Res. 113 (6), 746–753. https://doi.org/10.1016/j.mycres.2009.02.010.
Brainina, Khiena, Stozhko, Natalia, Vidrevich, Marina, 2019. Antioxidants: terminology, methods, and future considerations. Antioxidants (Basel, Switzerland) 8 (8). https://doi.org/10.3390/antiox8080297.
Bustin, S.A., Benes, Vladimir, Garson, J.A., Hellemans, Jan, Huggett, Jim, Kubista, Mikael, Mueller, Reinhold, et al., 2009. The MIQE guidelines: minimum information for publication of quantitative real-time PCR Experiments. Clin. Chem. 55 (4), 611–622. https://doi.org/10.1373/clinchem.2008.112797.
Calderon Flores, P., Yoon, J.S., Kim, D.Y., Seo, Y.W, 2021. Effect of chilling acclimation on germination and seedlings response to cold in different seed coat colored wheat (Triticum aestivum L.). BMC Plant Biol. 21 (1), 1–13. https://doi.org/10.1186/s12870-021-03036-z.
Chomczynski, Piotr, Wilfinger, William, Kennedy, Amy, Rymaszewski, Michal, Mackey, Karol, 2010. RNAzol® RT: a New Single-Step Method for Isolation of RNA. Nat. Methods 7 (12), 4–5. https://doi.org/10.1038/nmeth.f.315.
Conte, Paola, Piga, Antonio, Del Caro, Alessandra, Urgeghe, Pietro Paolo, Fadda, Costantino, 2021. Italian Dried Pasta: conventional and Innovative Ingredients and Processing. In: Boukid, Fatma (Ed.), Cereal-Based Foodstuffs: The Backbone of Mediterranean Cuisine. Springer International Publishing, Cham, pp. 89–116. https://doi.org/10.1007/978-3-030-69228-5_4 edited by.
Cory, Hannah, Passarelli, Simone, Szeto, John, Tamez, Martha, Mattei, Josiemer, 2018. The role of polyphenols in human health and food systems: a mini-review. Front Nutr. 5. https://doi.org/10.3389/fnut.2018.00087.
Daglia, Maria., 2012. Polyphenols as antimicrobial agents. Curr. Opin. Biotechnol. 23 (2), 174–181. https://doi.org/10.1016/j.copbio.2011.08.007.
Dhokane, Dhananjay, Karre, Shailesh, Kushalappa, A.C., McCartney, Curt, 2016. Integrated Metabolo-transcriptomics reveals fusarium head blight candidate resistance genes in wheat QTL-Fhb2. PLoS. One 11 (5), 1–27. https://doi.org/10.1371/journal.pone.0155851.
Dinelli, Giovanni, Segura Carretero, Antonio, Di Silvestro, Raffaella, Marotti, Ilaria, Fu, Shaoping, Benedettelli, Stefano, Ghiselli, Lisetta, Gutiérrez, Alberto Fernández, 2009. Determination of phenolic compounds in modern and old varieties of durum wheat using liquid chromatography coupled with time-of-flight mass spectrometry. J. Chromatogr. A 1216 (43), 7229–7240. https://doi.org/10.1016/j.chroma.2009.08.041.
Dong, Y., Xia, X., Ahmad, D., Wang, Y., Zhang, X., Wu, L., Jiang, P., Zhang, P., Yang, X., Li, G., He, Y., 2023. Investigating the resistance mechanism of wheat varieties to fusarium head blight using comparative metabolomics. Int. J. Mol. Sci. 24 (4). https://doi.org/10.3390/ijms24043214.
Doppler, Maria, Bueschl, Christoph, Ertl, Florian, Woischitzschlaeger, Jakob, Parich, Alexandra, Schuhmacher, Rainer, 2022. Towards a broader view of the metabolome: untargeted profiling of soluble and bound polyphenols in plants. Anal. Bioanal. Chem. 414 (25), 7421–7433. https://doi.org/10.1007/s00216-022-04134-z.
Dudonné, Stéphanie, Vitrac, Xavier, Coutière, Philippe, Woillez, Marion, Mérillon, Jean-Michel, 2009. Comparative study of antioxidant properties and total phenolic content of 30 plant extracts of industrial interest using DPPH, ABTS, FRAP, SOD, and ORAC Assays. J. Agric. Food Chem. 57 (5), 1768–1774. https://doi.org/10.1021/jf803011r.
Durazzo, Alessandra, Lucarini, Massimo, Souto, Eliana B, Cicala, Carla, Caiazzo, Elisabetta, Izzo, Angelo A, Novellino, Ettore, Santini, Antonello, 2019. Polyphenols: a concise overview on the chemistry, occurrence, and human health. Phytother. Res. 33 (9), 2221–2243. https://doi.org/10.1002/ptr.6419.
Enaru, Bianca, Drețcanu, Georgiana, Pop, T.D., Stănilă, Andreea, Diaconeasa, Zorița, 2021. Anthocyanins: factors affecting their stability and degradation. Antioxid. (Basel, Switzerland) 10 (12). https://doi.org/10.3390/antiox10121967.
Felici, L., Francesconi, S., Sestili, F., Balestra, G.M., 2024. Physiological and morphological traits associated with Fusarium head blight response in a flavonoid-rich durum wheat genotype. J. Plant Pathol. https://doi.org/10.1007/s42161-024-01663-7.
Feng, H., Li, S., Xue, L., An, L., Wang, X, 2007. The interactive effects of enhanced UV-B radiation and soil drought on spring wheat. South Afr. J. Botany 73 (3), 429–434. https://doi.org/10.1016/j.sajb.2007.03.008.
Flachowsky, Henryk, Szankowski, Iris, Fischer, Thilo C, Richter, Klaus, Peil, Andreas, Höfer, Monika, Dörschel, Claudia, et al., 2010. Transgenic apple plants overexpressing the *lc* gene of maize show an altered growth habit and increased resistance to apple scab and fire Blight. Planta 231 (3), 623–635. https://doi.org/10.1007/s00425-009-1074-4.
Francesconi, Sara, Balestra, Giorgio Mariano, 2020. The modulation of stomatal conductance and photosynthetic parameters is involved in fusarium head blight resistance in wheat. PLoS. One 15 (6 june), 1–21. https://doi.org/10.1371/journal.pone.0235482.
Francesconi, Sara, Steiner, Barbara, Buerstmayr, Hermann, Lemmens, Marc, Sulyok, Michael, Balestra, G.M., 2020. Chitosan hydrochloride decreases *fusarium graminearum* growth and virulence and boosts growth, development and systemic acquired resistance in two durum wheat genotypes. Molecules. 1–29. https://doi.org/10.3390/molecules25204752.
Funnell-Harris, D.L., Sattler, S.E., Dill-Macky, R., Wegulo, S.N., Duray, Z.T., O'Neill, P. M., Gries, T., Masterson, S.D., Graybosch, R.A., Mitchell, R.B., 2024. Responses of wheat (Triticum aestivum L.) constitutively expressing four different monolignol biosynthetic genes to Fusarium head blight caused by Fusarium graminearum. Phytopathology® https://doi.org/10.1094/PHYTO-01-24-0005-R.
Gaikpa, David Sewordor, Lieberherr, Bärbel, Maurer, Hans Peter, Friedrich H Longin, C., Miedaner, Thomas, 2020. Comparison of rye, triticale, durum wheat and bread wheat genotypes for fusarium head blight resistance and deoxynivalenol contamination. Plant Breed. 139 (2), 251–262. https://doi.org/10.1111/pbr.12779.
Gauthier, Léa, Marie-Noelle Bonnin-Verdal, Gisèle Marchegay, Laetitia Pinson-Gadais, Ducos, Christine, Florence Richard-Forget, Vessela, Atanasova-Penichon, 2016. Fungal Biotransformation of Chlorogenic and Caffeic Acids by Fusarium Graminearum: New Insights in the Contribution of Phenolic Acids to Resistance to Deoxynivalenol Accumulation in Cereals. International Journal of Food Microbiology 221, 61–68. https://doi.org/10.1016/j.ijfoodmicro.2016.01.005.
Gautier, Charlotte, Pinson-Gadais, Laetitia, Verdal-Bonnin, Marie Noelle, Ducos, Christine, Tremblay, Judith, Chéreau, Sylvain, Atanasova, Vessela, Richard-Forget, Florence, 2020. Investigating the efficiency of hydroxycinnamic acids to inhibit the production of enniatins by *fusarium avenaceum* and modulate the expression of enniatins biosynthetic genes. Toxins. (Basel) 12 (12), 1–17. https://doi.org/10.3390/toxins12120735.
Gebhardt, Y.H., Witte, Simone, Steuber, Holger, Matern, Ulrich, Martens, Stefan, 2007. Evolution of flavone synthase i from parsley flavanone 3beta-hydroxylase by site-directed mutagenesis. Plant Physiol. 144 (3), 1442–1454. https://doi.org/10.1104/pp.107.098392.
Golkari, Saber, Gilbert, Jeannie, Prashar, Suvira, Douglas Procunier, J., 2007. Microarray analysis of *fusarium graminearum*-induced wheat genes: identification of organ-specific and differentially expressed genes. Plant Biotechnol. J. 5 (1), 38–49. https://doi.org/10.1111/j.1467-7652.2006.00213.x.
Gondor, O.K., Szalai, G., Kovács, V., Janda, T., Pál, M., 2014. Impact of UV-B on drought- or cadmium-induced changes in the fatty acid composition of membrane lipid fractions in wheat. Ecotoxicol. Environ. Saf. 108, 129–134. https://doi.org/10.1016/j.ecoenv.2014.07.002.
Goujon, Thomas, Sibout, Richard, Eudes, Aymerick, MacKay, John, Jouanin, Lise, 2003. Genes Involved in the Biosynthesis of Lignin Precursors in Arabidopsis Thaliana. Plant Physiol. Biochem. 41 (8), 677–687. https://doi.org/10.1016/S0981-9428(03)00095-0.
Gozzi, M., Blandino, M., Dall'Asta, C., Martinek, P., Bruni, R., Righetti, L., 2023. Anthocyanin content and fusarium mycotoxins in pigmented wheat (triticum aestivum l. spp. aestivum): an open field evaluation. Plants 12 (4). https://doi.org/10.3390/plants12040693.
Gunnaiah, Raghavendra, Kushalappa, A.C., 2014. Metabolomics deciphers the host resistance mechanisms in wheat cultivar sumai-3, against trichothecene producing and non-producing isolates of *fusarium graminearum*. Plant Physiol. Biochem. 83, 40–50. https://doi.org/10.1016/j.plaphy.2014.07.002.
Gunnaiah, Raghavendra, Kushalappa, Ajjamada C., Duggavathi, Raj, Fox, Stephen, Somers, D.J., 2012. Integrated metabolo-proteomic approach to decipher the mechanisms by which wheat Qtl (Fhb1) contributes to resistance against *fusarium Graminearum*. PLoS. One 7 (7). https://doi.org/10.1371/journal.pone.0040695.
Hammer, Øyvind, Harper, D.A.T., 2005. Basic Statistical Methods. Paleontological Data Analysis, pp. 8–60. https://doi.org/10.1002/9780470750711.ch2.
Hao, Guixia, Naumann, Todd A., Vaughan, M.M., McCormick, Susan, Usgaard, Thomas, Kelly, Amy, Ward, Todd J., 2019. Characterization of a *Fusarium Graminearum* salicylate hydroxylase. Front. Microbiol. 10 (JAN), 1–11. https://doi.org/10.3389/fmicb.2018.03219.
Hao, Yuanfeng, Rasheed, Awais, Zhu, Zhanwang, Wulff, Brande B H, He, Zhonghu, 2020. Harnessing wheat fhb1 for fusarium resistance. Trends Plant Sci. 25 (1), 1–3. https://doi.org/10.1016/j.tplants.2019.10.006.
Hassan, Ali, Akram, Waheed, Rizwana, Humaira, Aftab, Zill-e-Huma, Hanif, Sana, Anjum, Tehmina, Alwahibi, Mona S, 2023. The imperative use of bacillus

consortium and quercetin contributes to suppress fusarium wilt disease by direct antagonism and induced resistance. Microorganisms. https://doi.org/10.3390/microorganisms11102603.
Hong, M.J., Ko, C.S., Kim, J.B., Kim, D.Y., 2024. Identification and transcriptomic profiling of salinity stress response genes in colored wheat mutant. PeerJ. 12. https://doi.org/10.7717/PEERJ.17043.
Hu, Chun, Cai, Yi-Zhong, Li, Wende, Corke, Harold, Kitts, David D, 2007. Anthocyanin characterization and bioactivity assessment of a dark blue grained wheat (*triticum aestivum* l. Cv. Hedong Wumai) extract. Food Chem. 104 (3), 955–961. https://doi.org/10.1016/j.foodchem.2006.12.064.
Huang, Junli, Gu, Min, Lai, Zhibing, Fan, Baofang, Shi, Kai, Zhou, Yan-Hong, Yu, Jing-Quan, Chen, Zhixiang, 2010. Functional analysis of the arabidopsis pal gene family in plant growth, development, and response to environmental stress. Plant Physiol. 153 (4), 1526–1538. https://doi.org/10.1104/pp.110.157370.
Jiang, Wenhui, Liu, Tianxiang, Nan, Wenzhi, Chamila Jeewani, Diddugodage, Niu, Yanlu, Li, Chunlian, Wang, Yong, et al., 2018. Two transcription factors tappm1 and tappb1 co-regulate anthocyanin biosynthesis in purple pericarps of wheat. J. Exp. Bot. 69 (10), 2555–2567. https://doi.org/10.1093/jxb/ery101.
Kage, Udaykumar, Hukkeri, Shivappa, Kushalappa, Ajjamada C, 2018. Liquid Chromatography and high resolution mass spectrometry-based metabolomics to identify quantitative resistance-related metabolites and genes in wheat QTL-2DL against Fusarium Head Blight. Eur. J. Plant Pathol. 151 (1), 125–139. https://doi.org/10.1007/s10658-017-1362-y.
Kikot, G.E., Hours, R.A., Alconada, Teresa Maria, 2009. Contribution of cell wall degrading enzymes to pathogenesis of *fusarium Graminearum*: a review. J. Basic Microbiol. 49 (3), 231–241. https://doi.org/10.1002/jobm.200800231.
Kurechi, TSUTAO, Kikugawa, KIYOMI, Kato, TETSUTA, 1980. Studies on the Antioxidants. XIII. Hydrogen Donating Capability of Antioxidants to 2, 2-Diphenyl-1-Picrylhydrazyl. Chem. Pharmace. Bull. 28 (7), 2089–2093. https://doi.org/10.1248/cpb.28.2089.
Kutmon, Martina, Iersel, Martijn P van, Bohler, Anwesha, Kelder, Thomas, Nunes, Nuno, Pico, Alexander R, Evelo, Chris T, 2015. PathVisio 3: an Extendable Pathway Analysis Toolbox. PLoS Comput. Biol. 11 (2), e1004085. https://doi.org/10.1371/journal.pcbi.1004085.
Lalak-Kańczugowska, Justyna, Witaszak, Natalia, Waśkiewicz, Agnieszka, Bocianowski, Jan, Stępień, Łukasz, 2023. Plant metabolites affect fusarium proliferatum metabolism and in vitro fumonisin biosynthesis. Int. J. Mol. Sci. https://doi.org/10.3390/ijms24033002.
Lei, Kai Jian, Zhang, Li, Du, Xiao Yu, An, Yi, Chang, Gai Hong, An, Guo Yong, 2018. A Chalcone Synthase controls the verticillium disease resistance response in both arabidopsis thaliana and cotton. Eur. J. Plant Pathol. 152 (3), 769–781. https://doi.org/10.1007/s10658-018-1521-9.
Li, Jingchong, Geng, Runlian, Kong, Xiangjun, Li, Lijie, Zhang, Zhiyong, Liu, Runqiang, 2023a. Transcriptomic and Physiological Properties Reveal the Tolerance Mechanism to Difenoconazole Toxicity in Wheat (Triticum Aestivum L. Ecotoxicol. Environ. Saf. 255 (March). https://doi.org/10.1016/j.ecoenv.2023.114787.
Li, Xiao lan, LÜ, Xiang, WANG, Xiao hong, PENG, Qin, ZHANG, Ming sheng, REN, Ming jian, 2020a. Biotic and Abiotic Stress-Responsive Genes Are Stimulated to Resist Drought Stress in Purple Wheat. J .Integr. Agric. 19 (1), 33–50. https://doi.org/10.1016/S2095-3119(19)62659-6.
Li, Xiaorui, Zhang, Xu, Liu, Guangping, Tang, Yan, Zhou, Chunju, Zhang, Lixin, Lv, Jinyin, 2020b. The spike plays important roles in the drought tolerance as compared to the flag leaf through the phenylpropanoid pathway in wheat. Plant Physiol. Biochem. 152 (April), 100–111. https://doi.org/10.1016/j.plaphy.2020.05.002.
Li, Zhe, Ahammed, Golam Jalal, 2023b. Plant Stress Response and Adaptation via Anthocyanins: a Review. Plant Stress 10, 100230. https://doi.org/10.1016/j.stress.2023.100230.
Liu, Huimin, Liu, Zijin, Wu, Yu, Zheng, Lamei, Zhang, Genfa, 2021. Regulatory mechanisms of anthocyanin biosynthesis in apple and pear. Int. J. Mol. Sci. https://doi.org/10.3390/ijms22168441.
Ma, D., Sun, D., Wang, C., Li, Y., Guo, T., 2014. Expression of flavonoid biosynthesis genes and accumulation of flavonoid in wheat leaves in response to drought stress. Plant Physiol. Biochem. 80, 60–66. https://doi.org/10.1016/j.plaphy.2014.03.024.
Ma, Dongyun, Li, Yaoguang, Zhang, Jian, Wang, Chenyang, Qin, Haixia, Ding, Huina, Xie, Yingxin, Guo, Tiancai, 2016. Accumulation of phenolic compounds and expression profiles of phenolic acid biosynthesis-related genes in developing grains of white, purple, and red wheat. Front Plant Sci. 7 (APR2016), 1–11. https://doi.org/10.3389/fpls.2016.00528.
Makandar, R., Nalam, V.J., Lee, H., Trick, H.N., Dong, Y., Shah, J., 2011. Salicylic Acid Regulates Basal Resistance to Fusarium Head Blight in Wheat. Mol.Plant-Microbe Interact.® 25 (3), 431–439. https://doi.org/10.1094/MPMI-09-11-0232.
Mandalà, Giulia, Ceoloni, Carla, Busato, Isabella, Favaron, Francesco, Tundo, Silvio, 2021. Transgene pyramiding in wheat: combination of deoxynivalenol detoxification with inhibition of cell wall degrading enzymes to contrast fusarium head blight and crown rot. Plant Sci. 313, 111059. https://doi.org/10.1016/j.plantsci.2021.111059.
Martínez-Fraca, J., de la Torre-Hernández, M.E., Meshoulam-Alamilla, M., 2022. Search of resistance against fusarium ear rot: ferulic acid contents in maize pericarp are associated with antifungal activity and inhibition of fumonisin production. Front. Plant Sci. 13 (April), 1–11. https://doi.org/10.3389/fpls.2022.852257.
McMullen, Marcia, Bergstrom, Gary, De Wolf, Erick, Dill-Macky, Ruth, Hershman, Don, Shaner, Greg, Van Sanford, Dave, 2012. A unified effort to fight an enemy of wheat and barley: fusarium head blight. Plant Dis. 96 (12), 1712–1728. https://doi.org/10.1094/PDIS-03-12-0291-FE.
Mesterhazy, A., 2020. Updating the breeding philosophy of wheat to fusarium head blight (Fhb): resistance components, qtl identification, and phenotyping—A review. Plants 9 (12). https://doi.org/10.3390/plants9121702.
Metsalu, Tauno, Vilo, Jaak, 2015. ClustVis: a web tool for visualizing clustering of multivariate data using principal component analysis and heatmap. Nucleic Acids Res. 43 (W1), W566–W570. https://doi.org/10.1093/nar/gkv468.
Miedes, Eva, Vanholme, Ruben, Boerjan, Wout, Molina, Antonio, 2014. The role of the secondary cell wall in plant resistance to pathogens. Front. Plant Sci. 5 (AUG), 1–13. https://doi.org/10.3389/fpls.2014.00358.
Mielniczuk, Elżbieta, Skwaryło-Bednarz, Barbara, 2020. Fusarium head blight, mycotoxins and strategies for their reduction. Agronomy. MDPI AG. https://doi.org/10.3390/agronomy10040509.
Moreira, L.R.S., Filho, E.X.F., 2016. Insights into the Mechanism of Enzymatic Hydrolysis of Xylan. Appl. Microbiol. Biotechnol. 100 (12), 5205–5214. https://doi.org/10.1007/s00253-016-7555-z.
Niu, Y., Li, J., Sun, F., Song, T., Han, B., Liu, Z., Su, P., 2023. Comparative transcriptome analysis reveals the key genes and pathways involved in drought stress response of two wheat (Triticum aestivum L) varieties. Genomics 115 (5), 110688. https://doi.org/10.1016/j.ygeno.2023.110688.
Oufensou, Safa, Virgilio Balmas, Emanuela Azara, Davide Fabbri, M. Antonietta Dettori, Christoph Schu, Franz Zehetbauer, Joseph Strauss, Giovanna Delogu, and Quirico Migheli. 2020. "Naturally occurring phenols modulate vegetative growth and deoxynivalenol biosynthesis in *fusarium Graminearum*." https://doi.org/10.1021/acsomega.0c04260.
Patra, Barunava, Schluttenhofer, Craig, Wu, Yongmei, Pattanaik, Sitakanta, Yuan, Ling, 2013. Transcriptional regulation of secondary metabolite biosynthesis in plants. Biochimica et Biophysica Acta (BBA) - Gene Regulatory Mech. 1829 (11), 1236–1247. https://doi.org/10.1016/j.bbagrm.2013.09.006.
Paznocht, L., Kotíková, Z., Burešová, B., Lachman, J., Martinek, P., 2020. Phenolic acids in kernels of different coloured-grain wheat genotypes. Plant, Soil Environ. 66 (2), 57–64. https://doi.org/10.17221/380/2019-PSE.
Picot, A., Atanasova-Pénichon, V., Pons, S., Marchegay, G., Barreau, C., Pinson-Gadais, L., Roucolle, J., Daveau, F., Caron, D., Richard-Forget, F, 2013. Maize kernel antioxidants and their potential involvement in fusarium ear rot resistance. J. Agric. Food Chem. 61 (14), 3389–3395. https://doi.org/10.1021/jf4006033.
Prat, Noemie, Guilbert, Camille, Prah, Ursa, Wachter, Elisabeth, Steiner, Barbara, Langin, Thierry, Robert, Olivier, Buerstmayr, Hermann, 2017. QTL mapping of fusarium head blight resistance in three related durum wheat populations. Theoret. Appl. Genet. 130 (1), 13–27. https://doi.org/10.1007/s00122-016-2785-0.
Rivas-San Vicente, M., Plasencia, J., 2011. Salicylic acid beyond defence: its role in plant growth and development. J. Exp. Bot. 62 (10), 3321–3338. https://doi.org/10.1093/jxb/err031.
Saulnier, Luc, Guillon, Fabienne, Chateigner-Boutin, Anne Laure, 2012. Cell wall deposition and metabolism in wheat grain. J. Cereal Sci. 56 (1), 91–108. https://doi.org/10.1016/j.jcs.2012.02.010.
Savignac, J.-M., Atanasova, V., Chereau, S., Ducos, C., Gallegos, N., Ortega, V., Ponts, N., Richard-Forget, F, 2023. Carotenoids occurring in maize affect the redox homeostasis of fusarium Graminearum and its production of type b trichothecene mycotoxins: new insights supporting their role in maize resistance to Giberella ear rot. J. Agric. Food Chem. 71 (7), 3285–3296. https://doi.org/10.1021/acs.jafc.2c06877.
Schiavi, D., Ronchetti, R., Di Lorenzo, V., Salustri, M., Petrucci, C., Vivani, R., Giovagnoli, S., Camaioni, E., Balestra, G.M., 2022. Circular hazelnut protection by lignocellulosic waste valorization for Nanopesticides development. Appl. Sci. (Switzerland) 12 (5). https://doi.org/10.3390/app12052604.
Schmittgen, T.D., Livak, K.J., 2008. Analyzing real-time PCR data by the comparative C T method. Nat. Protoc. 3 (6), 1101–1108. https://doi.org/10.1038/nprot.2008.73.
Sharma, Saloni, Kumar, Ashish, Singh, Dalwinder, Kumari, Anita, Kapoor, Payal, Kaur, Satveer, Shreon, Bhawna, Garg, Monika, 2022. Integrated transcriptional and metabolomics signature pattern of pigmented wheat to insight the seed pigmentation and other associated features. Plant Physiol. Biochem. 189 (August), 59–70. https://doi.org/10.1016/j.plaphy.2022.08.008.
Shirai, A., Tanaka, A., 2024. Effects of ferulic acid combined with light irradiation on deoxynivalenol and its production in Fusarium graminearum. Fungal. Biol. 128 (2), 1684–1690. https://doi.org/10.1016/j.funbio.2024.02.003.
Shoeva, O.Y., Gordeeva, E.I., Arbuzova, V.S., Khlestkina, E.K., 2017. Anthocyanins participate in protection of wheat seedlings from osmotic stress. Cereal Res. Commun. Cereal Res. Commun. 45 (1), 47–56. https://doi.org/10.1556/0806.44.2016.044.
Singh, Manisha, Thrimawithana, Thilini, Shukla, Ravi, Adhikari, Benu, 2020. Managing obesity through natural polyphenols: a review. Future Foods. 1–2 (September), 100002. https://doi.org/10.1016/J.FUFO.2020.100002.
Sivankalyani, Velu, Feygenberg, Oleg, Diskin, Sonia, Wright, Ben, Alkan, Noam, 2016. Increased Anthocyanin and flavonoids in mango fruit peel are associated with cold and pathogen resistance. Postharvest Biol. Technol. 111, 132–139. https://doi.org/10.1016/j.postharvbio.2015.08.001.
Sorahinobar, Mona, Niknam, Vahid, Ebrahimzadeh, Hassan, Soltanloo, Hassan, Behmanesh, Mehrdad, Enferadi, Sattar Tahmasebi, 2016. Central role of salicylic acid in resistance of wheat against *Fusarium Graminearum*. J. Plant Growth Regul. 35 (2), 477–491. https://doi.org/10.1007/s00344-015-9554-1.
Steiner, Barbara, Kurz, Harald, Lemmens, Marc, Buerstmayr, Hermann, 2009. Differential gene expression of related wheat lines with contrasting levels of head blight resistance after *fusarium Graminearum* inoculation. Theoret. Appl. Genet. 118 (4), 753–764. https://doi.org/10.1007/s00122-008-0935-8.

Su, P., Jiang, C., Qin, H., Hu, R., Feng, J., Chang, J., Yang, G., He, G., 2019. Identification of potential genes responsible for thermotolerance in wheat under high temperature stress. Genes. (Basel) (2), 10. https://doi.org/10.3390/genes10020174.

Sunil, L., Shetty, Nandini P, 2022. Biosynthesis and regulation of anthocyanin pathway genes. Appl. Microbiol. Biotechnol. 106 (5), 1783–1798. https://doi.org/10.1007/s00253-022-11835-z.

Tenea, Gabriela N, Bota, Adrian Peres, Cordeiro Raposo, Fernando, Maquet, Alain, 2011. Reference genes for gene expression studies in wheat flag leaves grown under different farming conditions. BMC Res. Notes 4 (1), 373. https://doi.org/10.1186/1756-0500-4-373.

Tomassini, A., Sella, L., Raiola, A., D'Ovidio, R., Favaron, F., 2009. Characterization and expression of *fusarium Graminearum* endo-polygalacturonases in vitro and during wheat infection. Plant Pathol. 58 (3), 556–564. https://doi.org/10.1111/j.1365-3059.2008.02019.x.

Trávníčková, M., Chrpová, J., Palicová, J., Kozová, J., Martinek, P., and Hnilička, F. (2024). Association between Fusarium head blight resistance and grain colour in wheat (Triticum aestivum L.). *Cereal Res. Commun.*, 0123456789. https://doi.org/10.1007/s42976-024-00514-6.

Tundo, Silvio, Janni, Michela, Moscetti, Ilaria, Mandalà, Giulia, Savatin, Daniel, Blechl, Ann, Favaron, Francesco, D'Ovidio, Renato, 2016. PvPGIP2 accumulation in specific floral tissues but not in the endosperm limits *fusarium Graminearum* infection in wheat. Mol. Plant-Microbe Interact. : MPMI 29 (10), 815–821. https://doi.org/10.1094/MPMI-07-16-0148-R.

Wagay, Nasir Aziz, Lone, Rafiq, Rafiq, Shah, Bashir, Sheikh Ummar, 2020. Phenolics: a game changer in the life cycle of plants. In: Lone, Rafiq, Shuab, Razia, Kamili, Azra N (Eds.), Plant Phenolics in Sustainable Agriculture : Volume 1. Springer Singapore, Singapore, pp. 241–275. https://doi.org/10.1007/978-981-15-4890-1_11 edited by.

Walter, S., Nicholson, P., Doohan, F.M., 2010. Action and reaction of host and pathogen during Fusarium head blight disease. New Phytol. 185, 54–66. https://doi.org/10.1111/j.1469-8137.2009.03041.x.

Wang, Jinxing, Liang, Jidong, Gao, Sha, 2018. Biodegradation of lignin monomers vanillic, p-coumaric, and syringic acid by the bacterial strain, sphingobacterium Sp. HY-H. Curr. Microbiol. 75 (9), 1156–1164. https://doi.org/10.1007/s00284-018-1504-2.

Wang, Lan, Yao, Yang, He, Zhonghu, Wang, Desen, Liu, Aihua, Zhang, Yong, 2013. Determination of phenolic acid concentrations in wheat flours produced at different extraction rates. J. Cereal Sci. 57 (1), 67–72. https://doi.org/10.1016/j.jcs.2012.09.013.

Wegener, Christina B, Jansen, Gisela, 2007. Soft-Rot resistance of coloured potato cultivars (Solanum Tuberosum L.): the Role of anthocyanins. Potato Res. 50 (1), 31–44. https://doi.org/10.1007/s11540-007-9027-4.

Wei, Q., Zhang, F., Sun, F., Luo, Q., Wang, R., Hu, R., Chen, M., Chang, J., Yang, G., He, G., 2017. A wheat MYB transcriptional repressor TaMyb1D regulates phenylpropanoid metabolism and enhances tolerance to drought and oxidative stresses in transgenic tobacco plants. Plant Sci. 265 (March), 112–123. https://doi.org/10.1016/j.plantsci.2017.09.020.

Whitney, K., Gracia-Gomez, G., Anderson, J.A., Simsek, S., 2022. Time course metabolite profiling of fusarium head blight-infected hard red spring wheat using ultra-high-performance liquid chromatography coupled with quadrupole time of flight/MS. J. Agric. Food Chem. 70 (13), 4152–4163. https://doi.org/10.1021/acs.jafc.1c08374.

Wiwart, Marian, Suchowilska, Elżbieta, Stuper-Szablewska, Kinga, Przybylska, Anna, Wachowska, Urszula, Gontarz, Dariusz, 2024. Variation in the Concentrations of Phenolic Compounds and Carotenoids in the Grain of a Large Collection of *Triticum Durum* Desf. Accessions. J. Cereal Sci. 116 (November 2023). https://doi.org/10.1016/j.jcs.2023.103842.

Wu, Fan, Zhou, Yao, Shen, Yingying, Sun, Zhengxi, Li, Lei, Li, Tao, 2022. Linking multi-omics to wheat resistance types to fusarium head blight to reveal the underlying mechanisms. Int. J. Mol. Sci. 23 (4). https://doi.org/10.3390/ijms23042280.

Yang, Wen-Jing, Du, Yong-Tao, Zhou, Yong-Bin, Chen, Jun, Xu, Zhao-Shi, Ma, You-Zhi, Chen, Ming, Min, Dong-Hong, 2019. Overexpression of TaCOMT improves melatonin production and enhances drought tolerance in transgenic Arabidopsis. Int. J. Mol. Sci. https://doi.org/10.3390/ijms20030652.

Zhang, Bixia, Lewis, K.M., Abril, Alejandra, Davydov, D.R., Vermerris, Wilfred, Sattler, S. E., Kang, Chulhee, 2020. Structure and function of the cytochrome p450 monooxygenase cinnamate 4-hydroxylase from sorghum bicolor. Plant Physiol. 183 (3), 957–973. https://doi.org/10.1104/pp.20.00406.

Zhang, Yang, Butelli, Eugenio, De Stefano, Rosalba, Schoonbeek, Henk-jan, Magusin, Andreas, Pagliarani, Chiara, Wellner, Nikolaus, et al., 2013. Anthocyanins double the shelf life of tomatoes by delaying overripening and reducing susceptibility to gray mold. Curr. Biol. 23 (12), 1094–1100. https://doi.org/10.1016/j.cub.2013.04.072.

Zhong, Qinling, Hu, Hongliang, Fan, Baofang, Zhu, Cheng, Chen, Zhixiang, 2021. Biosynthesis and roles of salicylic acid in balancing stress response and growth in plants. Int. J. Mol. Sci. https://doi.org/10.3390/ijms222111672.

Lanfei, Zhao, Peisen, Su, Bingqian, Hou, Hongyan, Wu, Yanhui, Fan, Wen, Li, Jinxiao, Zhao, et al., 2022. The Black Necrotic Lesion Enhanced Fusarium Graminearum Resistance in Wheat. Front. Plant Sci. 13, 1–15. https://doi.org/10.3389/fpls.2022.926621.

Singleton, V.L., Rossi, Joseph A., 1965. Colorimetry of Total Phenolics with Phosphomolybdic-Phosphotungstic Acid Reagents. AJEV 16 (3), 144–165. http://www.ajevonline.org/content/16/3/144.abstract.